 doi:10.20944/preprints202209.0459.v1

*Review*

# Advancement of Magnesium and Aluminum Alloys in the Role of Additive Manufacturing

**Sachin Kumar Sharma[1], Harpreet Singh Grewal[1], Kuldeep Kumar Saxena[2], Kahtan A. Mohammed[3], Chander Prakash[4*], J.P. Davim[5], Dharam Buddhi[6], Ramesh Raju[7], Dhanesh G. Mohan[8*], and Jacek Tomków[9]**

[1]Surface Science and Tribology Lab, Department of Mechanical Engineering, Shiv Nadar University, Gautam Buddha Nagar, UP, India-201314; ss393@snu.edu.in , harpreet.grewal@snu.edu.in
[2]Department of Mechanical Engineering, GLA University, Mathura, India-281406; saxena0081@gmail.com
[3]Department of medical physics, Hilla University College, Babylon, Iraq; kahtan444@gmail.com
[4*]Division of Research and Development, Lovely Professional University, India; chander.21503@lpu.co.in, chander.mechengg@gmail.com
[5]Department of Mechanical Engineering, University of Aveiro, Campus Santiago, 3810-193 Aveiro, Portugal; pdavim@mec.ua.pt
[6]Division of Research & Innovation, Uttaranchal University, Uttarakhand, 248007, Dehradun, India; dbuddhi@gmail.com
[7]Department of Mechanical Engineering, Sree Vidyanikethan Engineering College (Autonomous), Tirupathi, Andhrapradesh; mrramesh2002@gmail.com
[8*]Department of Material Processing Engineering, Zhengzhou Research Institute of Harbin Institute of Technology, Zhengzhou, China; dhaneshgm@gmail.com, dhanesh@sdu.edu.cn
[9]Faculty of Mechanical Engineering and Ship Technology, Gdańsk University of Technology, Poland; jacek.tomkow@pg.edu.pl
*Corresponding author: chander.21503@lpu.co.in (C.P.);dhanesh@sdu.edu.cn (D.G.M.)

**Abstract:** Magnesium and Aluminum alloys continue to be important in the context of modern and lightweight technologies. With the advancement of additive manufacturing (AM), components can be produced directly in a net shape, widen up the usage of magnesium and aluminum alloys as well as holding new ideas for the application of unique physical structures made feasible by 3D printing. Laser-based approach, one of the metal additive manufacturing (AM) methods, enables the formation of arbitrary 3D structures. With promising findings, research in this area is advancing quickly, bringing up a variety of potential applications in both the scientific and industrial sectors. Complex structures can now be manufactured easily utilizing AM technologies to meet the prerequisite objectives like reduced part numbers, greater functionality, and lightweight, among others. AM has the ability to meet demands by lowering costs and speeding up the manufacturing process. Due to their popularity in numerous high-value applications, aluminum, and magnesium alloys are one of the key material systems being researched in the laser-based additive manufacturing approaches. The review here aims to comprehensively examine the additive manufacturing of magnesium and aluminum alloys, highlighting the influence of the laser-based additive manufacturing approach on the mechanical characteristics, microstructure, and tribological performance of magnesium and aluminum alloys.

**Keywords:** magnesium; aluminum; additive manufacturing; complex structure; mechanical characteristics; tribological performance

## 1. Introduction

Provided that a product is constructed layer by layer from three-dimensional (3D) data, additive manufacturing (AM) approaches are frequently referred to as layer-by-layer manufacturing [1-3]. Fabricating geometrically complicated objects by utilizing a variety of AM technologies is increasingly profitable for the industry [2]. These approaches have the ability to meet demands by lowering the time from design to manufacture by substituting a single production procedure followed by a finishing step for a number of production procedures. Additionally, this satisfies manufacturers' desire to reduce lead

 doi:10.20944/preprints202209.0459.v1

times and supply chains. Since only the material required to create the desired product is used, or waste is avoided, several AM approaches offer the benefit of potential raw material savings [3-5]. It encourages the creation of hybrid materials and cost-effective parts and products that can achieve functionalities that are currently not possible [6]. Businesses worldwide are prompted and benefitted from the advancement in the field of additive manufacturing. Despite its benefits, it cannot be assumed that it would be appropriate and/or practical for enterprises of all shapes and sizes without taking complexity, customization, and production volume into account. Depending on the particular AM approach under investigation, there are distinct tiers of advantages that designers can take advantage of through either the evolutionary design of already existing products or revolutionary approaches that impart functionality that is not possible with conventional manufacturing techniques [7]. The capacity to incorporate complexity that is largely cost-insensitive is one of the main benefits of using AM, which is why design flexibility is the main justification for its use. This includes the capability to provide design features that are not possible traditionally, such as embedding complicated internal structures or channels into designs (lattices); enabling light-weighting through topology optimization; and ultimately, the production of multi-material, multifunctional devices. Combining components into assemblies has another benefit, reducing the need for mechanical fixtures and extra production processes [8].

Polymers, metals, and ceramics are just a few of the materials that can be used in AM technology. Among these materials, metallic materials are attracting more attention from the research and industrial point of view. For instance, Debroy et al. [9] revealed metallic printed materials' microstructures, flaws, and mechanical characteristics. Yakout et al. [10] depicted that the mechanical characteristics of various metallic alloys such as titanium and nickel alloy etc were affected by the process parameters of the 3D printing approach. Mg alloys are promising degradable biomaterial used for orthopedics, cardiology, respiratory, and urology [9-11]. The main benefit of Mg is that because the device totally disintegrates, long-term issues can be reduced or avoided. Another key benefit for orthopedics is that magnesium has modulus similar to bone, which reduces the negative effects originating from stress shielding [10]. Nevertheless, because of their relatively poor degrading characteristics (caused by the reactive nature of magnesium) and restricted formability, cast alloys have not been widely used in these applications (due to insufficient deformation modes and strong basal texture) [11-12]. Exploring the possibilities for alternate manufacturing methods to create the next generation of alloys with the desired physical qualities can therefore be important for a wide range of industries, from complicated lightweight consumer items to other developing technologies. For instance, the design flexibility of additive manufacturing can completely address the formability problem of Mg alloys since it allows for the manufacture of parts with near-net shapes and does not require further shaping or forming of the alloys [13]. Additionally, adjusting the process conditions can produce alloys with customized microstructures and property enhancements. The advancement of laser-based additively manufactured Mg alloys is discussed in detail marking the importance of lightweight complex parts and products formed in order to widen the usage of additive manufacturing.

Metal additive manufacturing technologies are evolving at a rapid pace due to the advancement of industrial applications that are easily accomplished with the usage and advantages offered by additive manufacturing approaches [15-16]. The processing parameters of laser-based additive manufacturing are obtained to be critical in order to maximize the usage of material in forming the product geometry. With the advancement in the technologies nationwide, additive manufacturing become the pre-requisite technology for researchers and industrialists. With the present need to develop lightweight alloys with complex and customized product formation geometry, the work-study revealed the advancements and recent developments related to laser-based additively manufactured Mg and Al alloys. The review article also highlights the number of alloys (Mg and Al) manufactured by the additive manufacturing approach. Though, currently, only a small number of Al and Mg alloys can be processed by laser-based additive manufacturing

 doi:10.20944/preprints202209.0459.v1

technologies. The related mechanical and tribological properties of Mg and Al alloy had been critically identified in the research studies. The challenges related to the fabrication of Mg and Al alloys were also discussed.

## 2. Advancement of Magnesium-based alloy in Additive Manufacturing

Magnesium alloys continue to be important in the context of modern and lightweight technologies. The increased use of Mg each year indicates a rise in demand for alloys containing Mg. With additive manufacturing (AM), components can be produced directly in a net shape, providing new ideas relating to the new prospects for Mg-based materials. The high feasibility of unique physical structures prepared by 3D printing widens the opportunities offering new advancements in the additively manufactured Mg alloys. Magnesium (Mg) is the least dense of the engineering metals (1.74g/cc), with densities that are roughly 65% lower than those of aluminum alloys, 38% lower than those of titanium, and 25% lower than those of steel [17-19]. Mg-based materials are desirable for lightweight applications in consumer electronics, aerospace, and automotive industries, resembling to high specific strength [20]. With suitable biodegradability, the elastic modulus of Mg-based alloys is quite similar to that of natural bone i.e., 45GPa [21-22] imparting protection against the stress shielding and providing sufficient healing to tissue. Mg-based materials are quite often found suitable for orthopedics in biomedical applications, such as fracture fixation, dynamic stability, joint replacement, cardiology, and maxillofacial applications [20-23]. Currently, casting (including precision die casting) accounts for more than 95% of the production of magnesium alloy products, whereas wrought magnesium alloys are only used in a restricted number of applications due to their poor formability and processability at room temperature [24-25].

Since additive manufacturing (AM) enables design capabilities that are not possible with traditional manufacturing and maybe also because material properties are still unknown, the interest in Mg alloys among the materials community is expanding. Additive manufacturing offers several exceptional benefits, including design freedom (topology optimization), little resource waste, and low energy consumption [26]. The drawback of traditional (formative or sub-tractive) fabrication routes is also eliminated by AM. The construction of precise geometrical characteristics like those seen in Figure. 1 is made possible by the capacity to produce complicated external and internal geometries with great accuracy [27]. With design flexibility, it is possible to optimize topology and use free space as a design variable to form the lightest engineering materials more-lighter. Furthermore, components having a big surface area, when utilized as biomaterials, enabled cell development, bone regeneration, and proliferation; alternatively, when employed as Mg electrodes, would offer a sizable reaction area [28]. The AM technique used for Mg-based materials is proved to be advantageous in fulfilling the rising demands for high-performance implants (biodegradable) for vascular and orthopedic surgery and making technological production more patient-specific and optimized the topological implants practically [27,29]. Additionally, the exact control of the process variables might result in alloys with custom microstructures and characteristics. Numerous AM techniques have been successfully used in recent studies to produce novel alloys with improved properties that are based on Al, Fe, and Ti [30-32]. However, there hasn't been much research done on AM-Mg alloys thus far. This may be partly because magnesium is reactive under air circumstances, which presents questions about health and safety as well as handling, oxidation, and evaporation of Mg-based materials. The research study from 2010 entails the controlling of risk factors while persisting with Laser-powder bed fusion (LPBF) as depicted in Figure. 2. The LPBF approach of additive manufacturing is extremely effective in preparing the additively manufactured Mg-based material products with greater accuracy by varying the compositions of the Mg alloys [27]. The required objective adheres to the current developments in AM-based Mg materials, thoroughly examining and evaluating the findings so far, and identifying the critical element that controls the overall characteristics of AM-based Mg materials.

 doi:10.20944/preprints202209.0459.v1

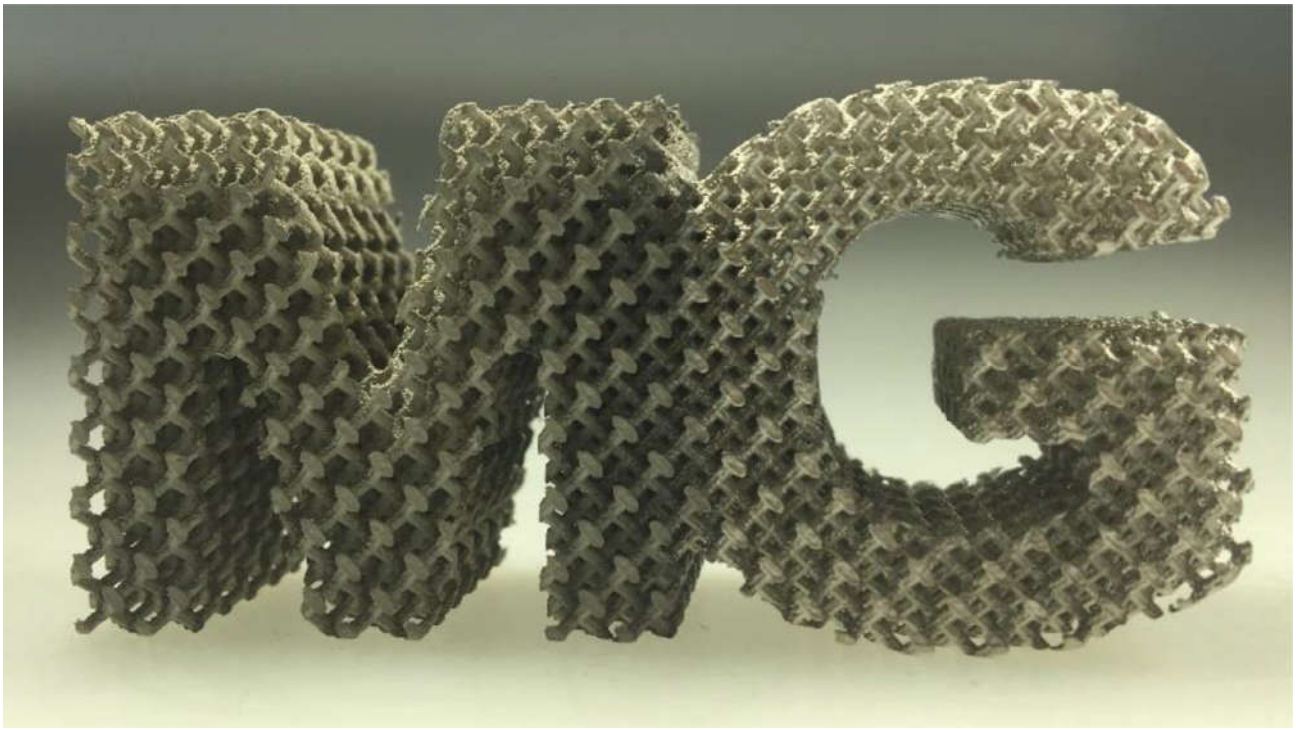

**Figure 1.** Laser powder-bed fusion (LPBF) created an "Mg"-shaped lattice structure in a magnesium alloy [27].

Preprints (www.preprints.org) | NOT PEER-REVIEWED | Posted: 29 September 2022 doi:10.20944/preprints202209.0459.v1

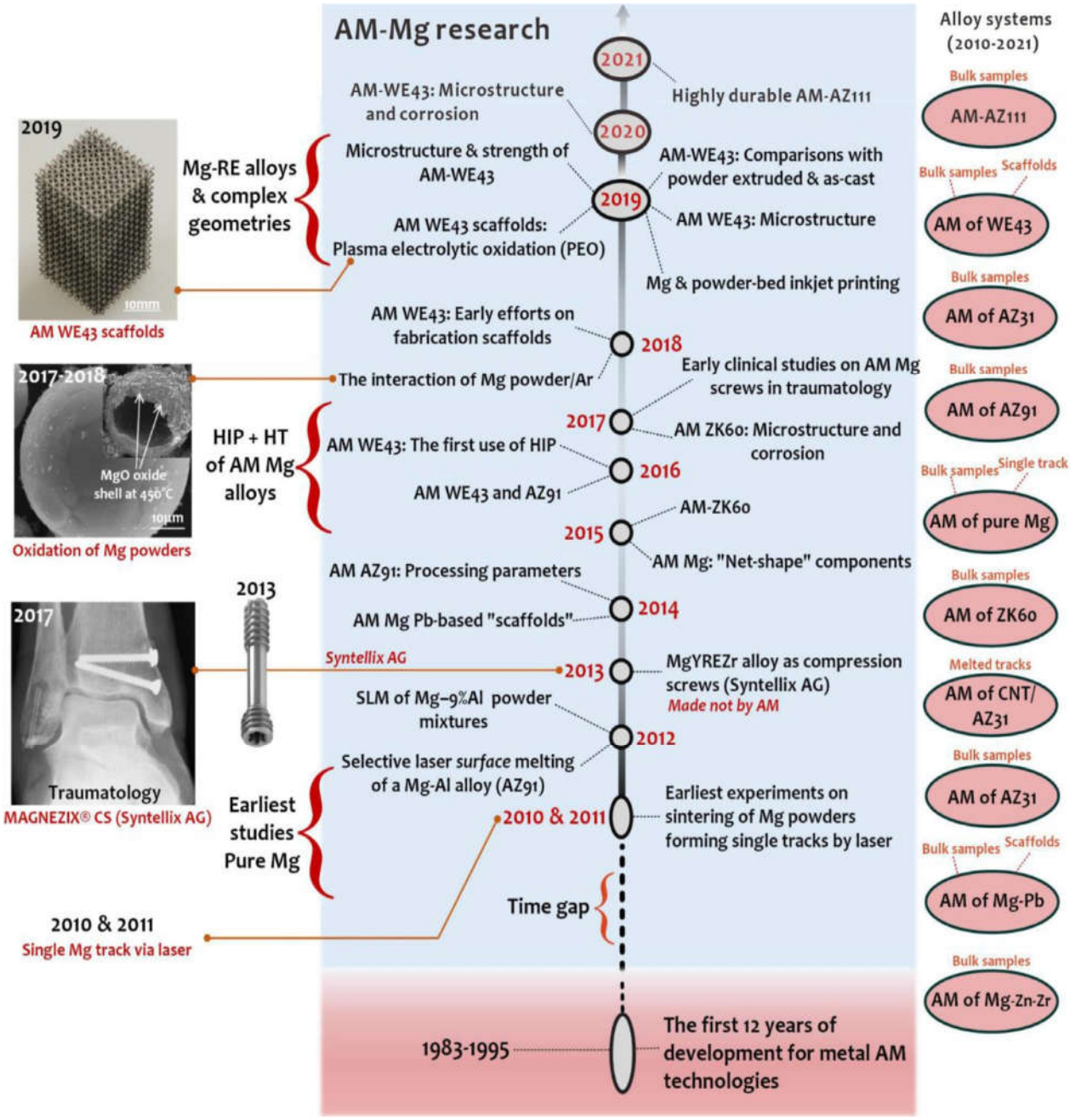


**Figure 2.** Advancement in the development of the Mg-based alloy via additive manufacturing (powder-based approach) [33].

*2.1. Laser-based additive manufacturing*

The most extensively researched energy source for AM-Mg is a laser, which offers certain distinct benefits over other energy sources. In order to melt the powder, lasers (high concentration of heat) are concentrated over the specified area of the powder bed for a short time duration. The molten powder is rapidly heated and quenched by this short-duration heat flux, which promotes fast solidification. The most extensively used additive manufacturing technique for magnesium alloys is attributed to LPBF, often recognized as SLM (Selective laser melting). Only a very small number of studies related to AM-based Mg materials are attributed to DLD (Direct laser deposition). Today, LPBF method is regarded as a potent and effective additive manufacturing technique for creating intricate 3D forms with high levels of precision and reproducibility together with acceptable metallurgical qualities [34-36]. Mg has an evaporation point of 1091 °C, while Al and Ti have evaporation points of 2470°C and 3287°C, respectively [37]. As a result, the

 doi:10.20944/preprints202209.0459.v1

temperature during LPBF will undoubtedly be higher than the temperature at which magnesium vaporizes, changing the composition of magnesium alloys generally. Systematically examining the evaporation during LPBF was done by We et al. [38]. It was discovered that the melting pool's rising temperature greatly quickens the rate at which magnesium burns. A number of processing variables, such as laser power, scan speed, hatch spacing, and layer thickness, have an impact on the melt pool's temperature. Porosity was regarded as the most critical issue while dealing with LPBF approach for Mg-based material that needs to address, in addition to evaporation. Table 1 summarises the impact of processing factors on porosity for magnesium particularly. It was discovered by analyzing the reference papers that LPBF powders are categorized as mixed Mg and Al powder, rather than Mg-Al powders that have already been pre-alloyed [39-43,27]. This indicates that achieving high relative density utilizing mixed elemental powders (metal) may be much more challenging, since the various thermal characteristics of each element may generate substantial local incompatibility in rapid cooling.

While some degree of porosity is acceptable because it is unavoidable, hot ripping and cracking must be avoided. The most serious problems that lower the as-built component's quality in LPBF are hot tearing and cracks [63-65]. In general aspect, low constitutional supercooling give rise to the formation of columnar grains columnar grains but temperature gradient is still substantial, making them particularly susceptible to hot ripping. Along with volumetric shrinkage during solidification, the thermal contraction between the columnar grains attributed to hot tearing and cavities formation resulting in enhancement in the length of columnar grains when temperature and liquid volume fraction drop [66]. No evidence related to the effects of processing parameters and alloying elements on hot tearing was evolved in Mg-based materials advancing to LPBF technique. Therefore, as per future aspect the alloying elements significance might consider to a better idea along with processing parameters identifying the behaviour of tearing in Mg materials. Empirically, an alloy (Mg-6Zn) having columnar grains and entails the high solidification range might be consider a more vulnerable one for cracking [67-70]. Furthermore, research can be accomplished in evaluating the fracture mechanism of additively manufactured Mg-based material identified as function of process parameter of LPBF and composition of alloy.

Preprints (www.preprints.org) | NOT PEER-REVIEWED | Posted: 29 September 2022 doi:10.20944/preprints202209.0459.v1

**Table 1.** Processing parameters of Mg-based alloy prepared by Additive Manufacturing powder-based approach.

| Alloy Components | Size and Shape (μm) of Powder | Methodology | Parameters used in powder-based additive manufacturing approach | | | | | Input Energy Density (J/mm³) | Relative Density (%) | Reference |
|---|---|---|---|---|---|---|---|---|---|---|
| | | | Power (W) | Spot size (μm) | Speed (mm/s) | Layer Thickness (μm) | Hatch Spacing (μm) | | | |
| Mg (Pure) | Pre-alloyed 24, spherical shape | Laser-powder bed fusion | 75 | 85 | 500 | 25 | 35 | 155 | 96.5 | [44] |
| | | | | | 1240 | | | 63 | 88.2 | |
| Mg (Pure) | Pre-alloyed 43, spherical shape | Laser-powder bed fusion | 85 | 90 | 90 | 25 | 90 | 290 | 96 | [45] |
| | | | 85 | | 100 | | | Less than 300 | | |
| Mg-9Al alloy | Blended Mg with size 42μm, irregular shape and Al 17μm, spherical shape | Laser-powder bed fusion | 10 | 30–75 | 10 | 50 | 80 | 250 | 74.5 | [46] |
| | | | 15 | | 20 | | | 187 | 78 | |
| | | | 15 | | 40 | | | 94 | 86.1 | |
| | | | 20 | | 40 | | | 125 | 82 | |
| Mg-9Al alloy | Blended Mg with size 24μm, spherical shape and Al 28μm, spherical shape | Laser-powder bed fusion | 70 | 80 | 500 | 30 | 30 | 156 | 95.7 | [47] |
| | | | | | 750 | | | 104 | 88 | |
| | | | | | 1000 | | | 78 | 83 | |
| | | | | | 1250 | | | 63 | 81 | |
| AZ61 alloy | Pre-alloyed with powder size 48μm, spherical shape | Laser-powder bed fusion | 145 | 75 | 300 | 45 | 65 | 210 | Less than 99 | [48] |
| | | | | | 350 | | | 181 | | |
| | | | | | 400 | | | 158 | | |
| | | | | | 450 | | | 141 | | |
| | | | | | 400 | | 85 | 157 | 99.1 | |
| | | | | | 400 | | 110 | 95 | 98.1 | |
| AZ61 alloy | Powder size with 70μm, spherical shape | Laser-powder bed fusion | 65 | 155 | 400 | 55 | 55 | 6000 | 77 | [49] |
| | | | 75 | | | | | 7000 | 89 | |
| | | | 85 | | | | | 8000 | 99 | |
| | | | 95 | | | | | 9000 | 95 | |
| AZ91 alloy | Powder size with 59μm, spherical shape | Laser-powder bed fusion | 210 | | 333 | 45 | 95 | 168 | 99.57 | [50] |
| AZ91 alloy | Powder size with 53-75μm, spherical shape | Laser-powder bed fusion | 125 | 85 | 10 | 355 | 510 | 70 | 96.62 | [51] |
| AZ91 alloy | Powder size with 25-63μm, spherical shape | Laser-powder bed fusion | 110 | 95 | 800 | 35 | 45 | 105 | Less than 99 | [52] |
| AZ91 alloy | Powder size with 30μm, spherical shape | Laser-powder bed fusion | 45 | – | 200 | 35 | 35 | 279 | 98 | [53] |
| AZ91/SiC composite | Powder size with 50nm, **SiC particles** | | | | | | | | 98.2 | |
| WE43 alloy | Powder size with 25μm, spherical shape | Laser-powder bed fusion | 125 | 95 | 960 | 35 | 45 | 105 | 98.5 | [33] |

 doi:10.20944/preprints202209.0459.v1

| | | | | | | | | | | |
|---|---|---|---|---|---|---|---|---|---|---|
| | Powder size with 30µm, spherical shape | | 145 | | 1200 | | | 105 | 99.1 | |
| | Powder size with 63µm, spherical shape | | 310 | | 1200 | | | 209 | 99.4 | |
| WE43 alloy | Powder size with 25-63µm, spherical shape | Laser-powder bed fusion | 205 | 95 | 700 | 35 | 45 | 239 | 99.78 | [54] |
| WE43 alloy | Powder size with 25-63µm, spherical shape | Laser-powder bed fusion | 205 | 75 | 1100 | 45 | 135 | 38 | 99.6 | [55] |
| WE43 alloy | Powder size with 25-63µm, spherical shape | Laser-powder bed fusion | 205 | 130 | 700 | 35 | 45 | 239 | 99.89 | [56] |
| WE43 alloy | Powder size with 25-63µm, spherical shape | Laser-powder bed fusion | 200 | 110 | 800 | 35 | 210 | 42 | 99.75 | [57] |
| | | | 200 | | 800 | | 245 | 35 | 98.4 | |
| | | | 200 | | 1200 | | 210 | 29 | 96.6 | |
| | | | 200 | | 1200 | | 210 | 20 | 87.7 | |
| G10K alloy | Powder size with 63µm, spherical shape | Laser-powder bed fusion | 85 | – | 200 | 35 | 90 | 135 | 99.3 | [58] |
| GZ112K alloy | Powder size with 31-44µm, spherical shape | Laser-powder bed fusion | 85 | 110 | 100 | 35 | 90 | 268 | 98.9 | [59] |
| | | | | | 300 | | | 90 | 99.8 | |
| | | | | | 500 | | | 54 | 99.4 | |
| | | | | | 700 | | | 39 | 99.5 | |
| | | | | | 1000 | | | 28 | 96.4 | |
| | | | | | 1500 | | | 19 | 71.9 | |
| | | | | | 500 | | 45 | 106 | 99.4 | |
| | | | | | 500 | | 145 | 37 | 96.4 | |
| GZ151K alloy | Powder size with 25-65µm, spherical shape | Laser-powder bed fusion | 210 | – | 700 | 35 | 75 | 138 | 98 | [60] |
| Mg-1Zn alloy | Blended Mg-5.5 Zn | Laser-powder bed fusion | 185 | 140 | 700 | 25 | 75 | 184 | 99.1 | [61] |
| Mg-2Zn alloy | Powder size with 36µm, spherical shape | | | | | | | | 98.5 | |
| Mg-6Zn alloy | Powder size with 31µm, spherical shape | | | | | | | | 94.9 | |
| Mg-12Zn alloy | Powder size with 19µm, spherical shape | | | | | | | | 99 | |
| ZK60 alloy | Powder size with 30µm, spherical shape | Laser-powder bed fusion | 210 | 140 | 300 | 25 | 85 | 418 | 95 | [62] |
| | | | | | 500 | | | 255 | 94 | |
| | | | | | 700 | | | 180 | 89 | |
| | | | | | 900 | | | 140 | 85 | |

*2.2. Investigation of Mg alloy via Additive Manufacturing*

Advancing to additive manufacturing approach for Mg-based materials, very few combinations has been studied while comparing to wrought and cast alloys. This is primarily due to the high expense of producing atomized pre-alloyed powder on a customized basis, which is highly expensive as compared to the customized composition of wrought and cast alloy. Pure magnesium, AZ91, and WE43 are now the most widely used compositions of magnesium-based materials used for additive manufacturing [71-76]. These alloys are attributed to superior printability, sustainable in structural and biological applications, and attracting the market demand (for being light weight). The detailed research outcomes of the various research studies has been compiled in the section below in order to identified the development relating the AM approach to Mg alloy. The study paved a way for the future research related to additively manufactured Mg-based materials.

 doi:10.20944/preprints202209.0459.v1

2.2.1. Pure Mg alloy

At initial stage the researcher, Ng et al. had examined the first experimental approach to produce the customized equipment using laser-based additive manufacturing approach relating the Mg-based material [77]. The Nd-YAG laser was used as a primarily source of heat to melt the powder over the powder bed in LPBF approach. For a single-track laser scan, several laser powers and scan speeds were tested during the initial research relating the Mg-based material to LPBF approach. The variation of laser power with scan speed were depicted in figure. 3(A) [77-78]. It was concluded from various research studied that LPBF approach of additive manufacturing does not accomplished with irregular and coarse powder. Other than that, LPBF approach holds the good accountability with spherical and atomized fine powder under the pre-requisite condition of processing parameters [77]. The variability of grain size with pure Mg obtained via LPBF was observed in the range of 2 to 5μm. To incorporate the such tiny grain size in pure Mg is quite a difficult task before advancing to the LPBF. Only extreme plastic deformation approach at low temperature condition were able to accommodate the such tiny grain size distribution in pure Mg materials [79-80]. Therefore, LPBF approach plays a significant role in refining the microstructure of material over traditional casting and thermomechanical processing. Furthermore, research studies identified that the LPBF single-track sample has an extremely high hardness as well as a significant density of cracks around the grain boundaries and formed the oxides layers around the boundary [81-83]. The researcher, Hu et al. developed the first bulk Mg relating to LPBF approach used in producing customized parts of Mg material. For spherical shape of powder, the high density of gas pores was obtained through LPBF approach, while irregular shape of powder marks the abundance of fusion pores, but resemble to the structure depicting certain interconnectivity between the pores [84-85]. Pure Mg material relating to additive manufacturing approach can be produced by DLD approach (Direct laser deposition) of additive manufacturing in addition to LPBF approach [86-87].

2.2.2. Mg-Al alloy

The most significant commercial composition of Mg-Al-based alloys in the cast and wrought forms is AZ31 [88-90]. While the majority of formation of AZ31 alloy based additively manufactured part is attributed to wire-arc approach but there is very little literature on laser-powder-based additive manufacturing. In actuality, high Al concentration Mg-Al alloys, such as AZ91, make up the majority of laser-based Mg-Al alloys [91]. This is because the addition of Al necessitates grain refinement of the alloys through superheating or inoculation, enhances castability (hence printability), and offers reinforcement through the solute and $Mg_{17}Al_{12}$ intermetallic phase [91-92]. Coming to the LPBF approach, Pawlak et al. investigated the fabrication of AZ31 alloy-based material parts via LPBF approach and attributed to the low porosity level around 0.5% [93]. In LPBF, AZ61 and AZ91 also attain such a low porosity level, proving the alloy's acceptable printability [27,94]. The AZ91 and AZ61 alloys forming through LPBF approach attributed to equiaxed and fine grain distribution, as well as attaining the texture that was almost randomly distributed [95-98]. Figure. 3B(a) marking the variation in the grain size distribution ranging from 1 to 3μm in Mg-Al alloy prepared via LPBF approach. According to some research, the β -$Mg_{17}Al_{12}$ intermetallic is primarily absent from the grain interior and is instead scattered along the grain boundaries and linked, as seen in Figure. 3B(b) [27]. However, some results display grains that are extended in the construction direction seen in Figure. 3B(c). While the intermetallic phase (β-$Mg_{17}Al_{12}$ ) finds around the grain boundary. Furthermore, research identified that there exist abundant spherical intermetallic (β -$Mg_{17}Al_{12}$) nanoparticles inside grain boundaries attaining the diameter around 300nm as identified in figure. 3B(d) [27].

Preprints (www.preprints.org) | NOT PEER-REVIEWED | Posted: 29 September 2022 doi:10.20944/preprints202209.0459.v1

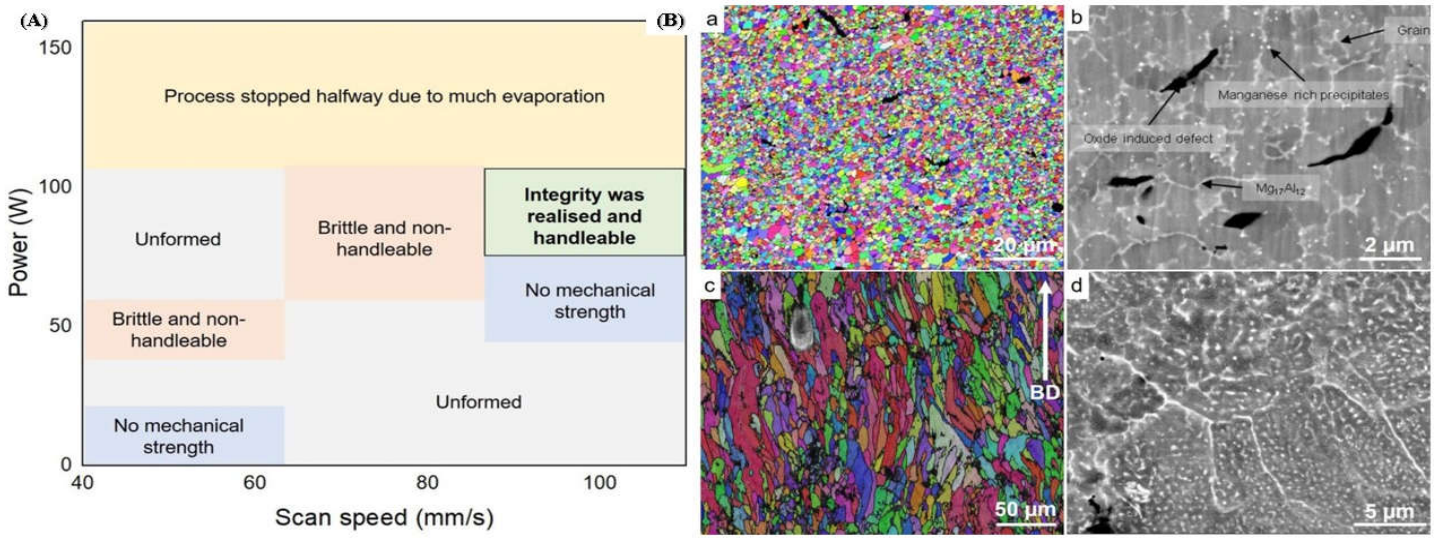


**Figure 3.** (A) Processing parameters of laser-based powder approach, (B) (a-c) depicted EBSD orientation, (b-c) SEM characterisation of AZ91 alloy formed by laser powder bed fusion [27].

2.2.3. Mg-RE alloy

The additively manufactured Mg-RE alloy has received the greatest attention for use in biomedical implants especially WE43 alloy. Although, WE43 alloy attain significant importance in biomedical application, but it also have good printability which accounts for new doorway in order to achieve the reduced porosity [99-100], better than AZ91 alloy as discussed in [93]. Being biocompatible, WE43 alloy does not cause any negative cell reactions such as cytotoxicity, whereas Aluminum in Mg-Al alloy accounted for cytotoxicity. Al is a neurotoxic element that is prohibited from bioabsorbable magnesium alloys due to the high concern relating to Alzheimer's disease. Consequently, WE43 alloy has garnered increased interest as a biodegradable implant material in scaffold applications [27]. Despite, very few grains with aberrant grain development during LPBF, Zumdick and Jauer's early tests of LPBF over WE43 showed the formation of equiaxed grains around the boundary and provides a pathway to the refinement in the grain size, depicted in Figure. 4(a) [27]. Intriguingly, the LPBF approach over WE43 alloy exhibited a completely different microstructure way-back in 2019 pertaining to the similar processing parameters illustrated by same research team, entailing the dominance of large, strongly basal-textured grains with irregular shapes [56]. Figure 4(b–d) shows that although the laser beam's quick solidification of the melt pool produces fine, columnar, equiaxed grains [33,56]. The succeeding laser scans in the LBPF process result in heat treatment, which leads to grain development with a distinct [0001]/BD texture. It is demonstrated that, following a single-layer deposition, there is significant grain development and that, following the formation of two layers, the grains achieve their maximum size. It is uncertain what precise mechanism results in such vast grain expansion and textural development. In contrast, no such grain development can be seen in Figure. 4(a) [27]. The authors suggested that yttrium oxide ($Y_2O_3$) particles, which are thought to offer Zener-pinning to inhibit grain formation, may be present in varying proportions in powders from various vendors [101-102]. In actuality, oxygen and the early RE elements have a strong affinity towards inhibiting the grain formation. In comparison to MgO (596 kJ/mol), the Gibbs free energy required for the production of $Y_2O_3$ and $Nd_2O_3$ is 1815 and 1806kJ/mol, respectively [27,103]. Therefore, a significant proportion of RE oxide has been present in all LPBF-WE43 publications to the date shown in Figure. 4(e-f) [56]. The big and basal-oriented grains are nonetheless predominant in the WE43 alloy formed by LPBF approach concluded by Esmaily et al., despite the high density of RE oxide that doubt the efficiency of RE oxide in preventing grain development from Zener Pinning [104-105]. In actuality, the concentration and types of solute particles are often referred to as the Growth Restriction Factor proposed by St

 doi:10.20944/preprints202209.0459.v1

John, have a greater impact on grain growth during solidification [106]. The Growth Restriction Factor (Q) in this model is

$$Q=C_0m(k-1)$$ [107];

where K relating to equilibrium distribution coefficient, $C_0$ related to composition of solute particles, and m relating to liquidus line slope.

A larger solute concentration causes a greater thermodynamic limit on grain development that has been observed in various research studies [108-110]. Therefore, the low concentration of solute particles relating to the RE element in the powder prevents the oxidation of WE43 alloy powder during production, transportation, and storage. Due to the inability of the low solute particle concentration in powder to prevent preferred development, the result is the massive, basally oriented grains as seen in Figure. 4(b-c) [56]. Therefore, researchers have customized the composition of powder and inherited various compositions resembling to Mg-Gd systems in addition to experiments based on commercial WE43 powder [111-112]. The as-LPBF Mg-Gd-based alloy incorporated the significant grain refinement (1-2μm), resemble equiaxed grain with random distribution of grains around the boundary [27]. The relative density of the alloy can reach 99.95% and it has few oxides and pores. Similar behaviour was obtained in DLD (Direct laser deposition) manufactured Mg-10Gd-3Y-0.4Zr alloy with spherical powder (100-300μm) pertaining to the randomness in the distribution of the equiaxed grains [27]. DLD reveals that the alloy sample has a bigger grain size and a higher pore percentage. Therefore, in order to limit the enhancement in the grain size of basal-oriented grains, the appropriate amount of Gd content (>10 wt. %) should be primarily used during solidification, irrespective of any approach used (DLD or LPBF) [113-114].

Preprints (www.preprints.org) | NOT PEER-REVIEWED | Posted: 29 September 2022 doi:10.20944/preprints202209.0459.v1

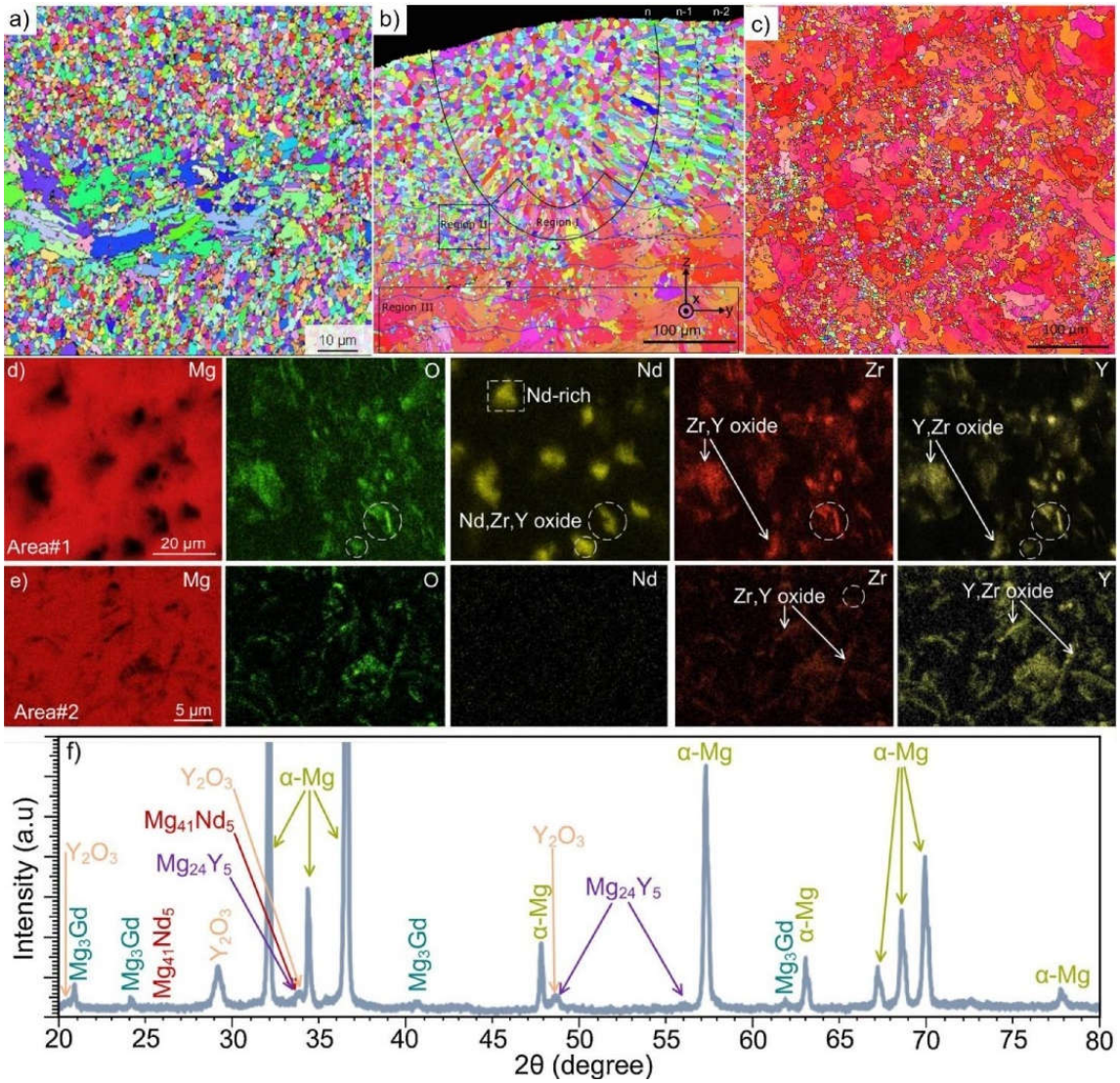


**Figure 4.** EBSD image shows equiaxed, fine, and random grain representation in (a) bulk LPBF-WE43, (b) last melt pool corresponds to basal- orientated, large, and irregular shape grains, (c) basal-orientated, large, irregular shape grains in the bulk sample, (d-e) EDS image at different magnification for same materials, and (f) XRD image depicted intermetallic and oxygen-rich elements in WE43 alloy [27, 33, 56].

2.2.4. Mg-Zn alloy

Despite Zn being biocompatible in nature, Advancement to Mg-Zn alloy has not been explored significant as comparable to Mg-RE and Mg-Al alloys. The research studies suggested that the wide range of solidification and low eutectic temperature (325°C) of Mg-Zn alloy, accounts for the poor printability as compared to Mg-RE and Mg-Al alloys [27]. Only at very low (less than 1wt.%) and very high (12wt.%) Zn concentrations will produce an acceptable level of porosity. Resembling to ZK60 alloy where Zn concentration opt at 6wt.%, the hot cracking and higher density of pores were accommodated in the additively manufactured ZK60 alloy [115,116]. As a result, the alloy is rendered useless and unusable. The research studies concluded that ZK60 alloy produced by LPBF approach produces the relative density around 97%. Therefore, the addition of Zn as an alloying element in the additively manufactured Mg-materials via laser-based approach adheres to the minimal quantity. In addition to the Mg-Zn, Mg-RE, and Mg-Al-based alloys, the research studies explored the Mg-Sn alloy with the blended powder and Mg-Ca alloy with pre-alloyed powder [27]. The outcomes depicted the short range of solidification and high value of eutectic temperature (466°C and 510°C for Mg-Sn and Mg-Ca alloy system)

 doi:10.20944/preprints202209.0459.v1

which accounts for the higher printability of these alloys as compared to Mg-Zn alloy [118]. Along with good printability, these alloys incorporated the equiaxed grain and prompted the refine of the microstructures. But for future perspective, more research needs to be carried out on these alloys via LPBF identifying the behaviour of solidification, the evolution of the microstructure, and the mechanical and electrochemical properties [118-122].

*2.3. Mechanical Properties of Laser-based Additive Manufacturing approach*

Accounting to the mechanical characteristics of additively manufactured Mg materials with laser-based approach, the research outcomes are concluded in the Table. 2 for future research perspective. The graphical variation in the yield strength with elongation (%) for various wrought alloys (extruded and rolled)and cast alloy is shown in in Figure. 5(a) [27]. For laser-based additively manufactured parts, the compression or hardness test are pre-requisite in order to analyse the mechanical behaviour of the AM-Mg alloy as prepared parts via LPBF accounts for the ductility less than 5%, while some of the alloys have none at all which is unacceptable for engineering material. Other than low ductility, Some alloys pertaining the weak texture, grains can be fine, or equiaxed, fine grains, and resemble to low porosity during the microstructure behaviour, irrespective of low ductility [123-125]. Low porosity accounts for the good printability for the alloying material. Furthermore, research studies were focussed in order to identified the reason of low ductility in laser-based additively manufactured Mg materials. Firstly, the quick solidification causes the as-LPBF to have significant residual stress, which lowers the alloy's ductility [124]. Secondly, the examined alloys such as Mg-Gd, WE43, and AZ91 alloys, include significant amounts of alloying elements addition incorporated the intermetallic phase around the grain boundaries. Therefore, due to the formation of intermetallic phase around the grain boundary, the brittle behaviour as well as local failure around grain boundaries were observed. The presence of local failure showcases the inability of material to cause the plastic deformation (twining and slipping around the boundary as well as sliding of grain boundary etc.). Low ductility encountered in the laser-based additively manufactured part was due to the poor redeposition of powder or vapor over the surface of parts that weakened the bond between the particles. The fracture surface's cauliflower-like characteristic is shown in Figure. 5(b). The WE43 alloy currently has the highest documented ductility among laser-additive produced magnesium alloys at 12.2% [27]. Despite the presence of some gas pores, the fracture surfaces were clearly visualized in Figure. 5(c) that the sample has broken in a ductile manner. High-temperature annealing approach can increase the ductility of an alloy. The enhancement in the ductility of WE43 alloy formed by LPBF encountered to 2.5% in as-built state to 4.5% after heat-treatment by annealing at 535 °C for 24 hours and aging at 205 °C for 48 hours [126]. FSP (Friction stir processing) dramatically reduces the residual stresses, grain size, and redistributed the intermetallic of Mg-10Gd-0.3Zr alloy, led to a more striking increase in ductility from 2.2 to 7.5% [27]. Although it is unlikely that the net shape component formed via LPBF approach will be produced by friction stir processing approach in actual applications of engineering showcasing that the alloy formed by LPBF approach is not inherently brittle in nature. Therefore, the optimization of processing parameters, composition of alloy, and quality of powder material used improves the ductility of additively manufactured Mg alloy by LPBF approach. The detailed description of the investigation of mechanical characteristics of Mg-based alloy prepared by powder-based fusion approach of additive manufacturing.

Preprints (www.preprints.org) | NOT PEER-REVIEWED | Posted: 29 September 2022 doi:10.20944/preprints202209.0459.v1

**Table 2.** Various properties of laser beam additively manufactured Mg-alloy.

| Alloy | Input Energy Density (J/mm³) | Grain Size (μm) | Microhardness (HV) | Yield Strength (MPa) | Ultimate Tensile Strength (MPa) | Elongation.(%) | Electrochemical Solution | $I_{corr}$ (μA/cm²) | Mass loss mm/year | References |
|---|---|---|---|---|---|---|---|---|---|---|
| Mg (Pure) | 97-88 | 1–5 | – | – | – | – | Hank's solution | 75-180 | 5-33 | [44] |
| Mg (Pure) | 295 | – | 52.4 | – | – | – | – | – | – | [45] |
| Mg-9Al | 251 | 15–25 | 71 | – | – | – | | – | – | [46] |
| Mg-9Al | 150 | 1.5–3.5 | | – | 274 | 1.1 | – | – | – | [47] |
| AZ61 | 140 | 1.5 | – | 220 | 275 | 3.5 | – | – | – | [48] |
| | 155 | 1.7 | | 235 | 285 | 3.0 | | | | |
| | 180 | 2.0 | | 220 | 260 | 2.9 | | | | |
| | 205 | 2.4 | | 214 | 240 | 2.2 | | | | |
| AZ61 | 125 | 4.5 | 71 | – | – | – | Simulated body fluid solution | | 2.8 | [49] |
| | 145 | 9 | 81 | | | | | | 2.5 | |
| | 161 | 10 | 94 | | | | | | 1.3 | |
| | 181 | 12 | 91 | | | | | | 1.6 | |
| AZ91 | 165-85 | 1.5-3 | 86-105 | 27 | 296 | 1.2 | | | | [50] |
| | 83 | 2.9 | | 237 | 254 | 1.8 | | | | |
| AZ91 | 68 | 1–11 | 114 | – | – | – | | | | [51] |
| AZ91 | 103 | 1–2 | – | 270 | 330 | 3.9 | | | | [52] |
| AZ91 | 280 | 3.5 | – | 310 | 350 | 1.1 | – | – | – | [53] |
| AZ91-SiC | 280 | 1.2 | – | 265 | 310 | 2.1 | – | – | – | |
| AZ91–2Ca | – | – | – | 240 | 335 | 3.3 | – | – | – | [27] |
| WE43 | 125 | 35 | – | – | – | – | NaCl (0.1M) | 5.1 | 6.1 | [27] |
| | 150 | 28 | | | | | | 5.0 | – | |
| | 300 | 19 | | | | | | 4.6 | | |
| WE43 | 240 | 1.5 | – | 300 | 310 | 12.1 | – | – | 7.3 | [54] |
| WE43 | 40 | 1–4 | – | 215 | 255 | 2.8 | – | – | – | [55] |
| WE43 | 240 | 20.5 | – | – | – | – | – | – | – | [56] |
| WE43 | | | | | | | | | | [57] |
| G10K | 135 | 28 | 81 | 187 | 230 | 2.3 | – | – | – | [58] |
| GZ112K | 90 | 1.8 | – | 330 | 335 | 4.2 | – | – | – | [59] |
| GZ151K | 140 | 2.1 | | 350 | 370 | 3..2 | – | – | – | [60] |
| Mg-1Zn | 185 | – | 52 | | 150 | 11.1 | – | – | – | [61] |
| Mg-2Zn | | | 45 | | 75 | 2.4 | | | | |
| Mg-6Zn | | | 66 | | 55 | 1.4 | | | | |
| Mg-12Zn | | | 84 | | 80 | 3.3 | | | | |
| ZK30 | 2002 | – | 81 | – | – | – | Simulated body fluid solution | 17.8 | 1.20 | [27] |
| ZK30-Cu | | | 99 | | | | | 47.8 | 2.25 | |
| Pure Mg | – | – | – | – | – | – | NaCl (3wt.%) | 999 | 144 | [27] |

Preprints (www.preprints.org) | NOT PEER-REVIEWED | Posted: 29 September 2022 doi:10.20944/preprints202209.0459.v1

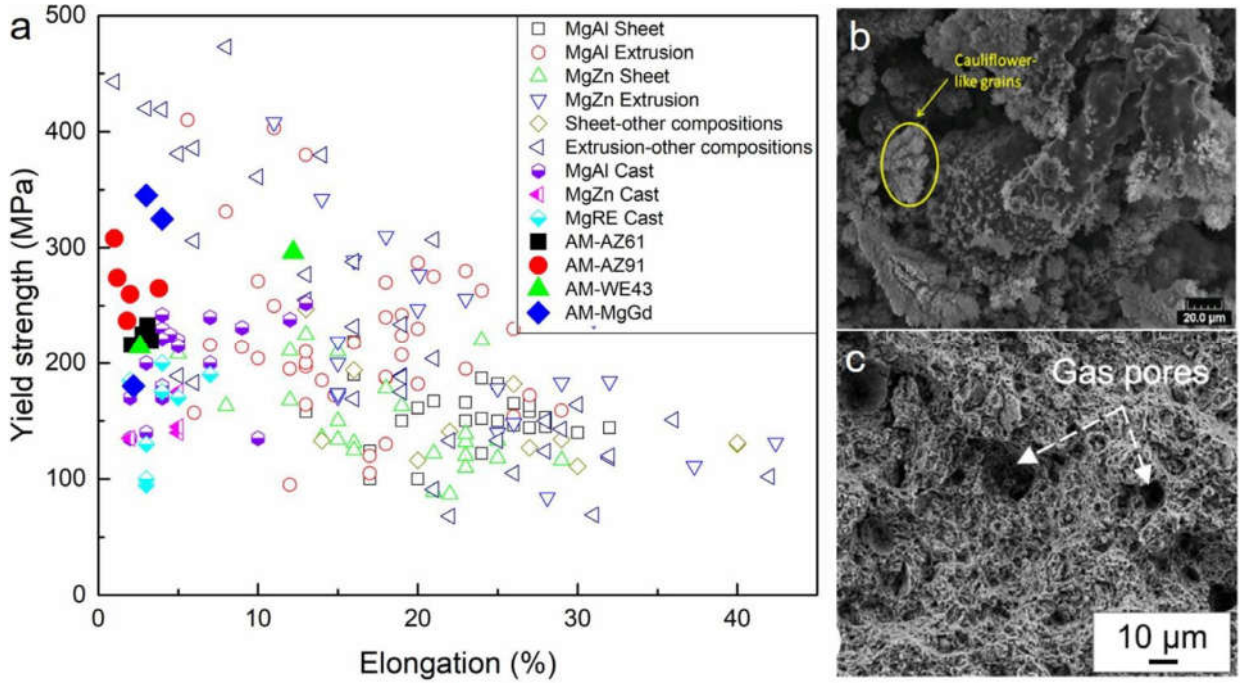


**Figure 5.** (a) Tensile characterization of additively manufactured Mg-based material via LPBF approach against wrought and cast alloys,(b-c) Fractured surface of (b) Mg-9Al alloy and (c) WE43 alloy [27, 54, 127].

2.3.2. Electrochemical durability of Mg-based alloy prepared by Lased-based powder fusion

Biodegradable implants are attributing to the most promising aspect for additively manufactured Mg-based materials. For better implantation outcome, oral and maxillofacial implants retained the sufficient mechanical integrity for the initial first month before gradually deteriorating, becoming completely dissolved and metabolized after three months [128]. Given that magnesium and its alloys are known to have low corrosion resistance in the majority of aqueous settings, this demands adequate electrochemical durability. With regard to LPBF approach, the corrosion current density ($I_{corr}$) of Mg (pure) in Hank's solution is far better than the cast Mg (pure) ingot tested under the same conditions (23.6μm/cm$^2$) and varies from 74 to 177μm/cm$^2$ [129]. Depending on the processing conditions, the mass loss rate ranges from 3 to 32mm/year. In a solution of 3 wt.% NaCl, the corrosion rate of pure Mg produced by DLD is about 144mm/year [27]. The loosely fused Mg clusters and sintered Mg powder provides the negative effect attributing to corrosion resistance. As a result of higher corrosion rate, the parts formed by LPBF approach inherited some defects, advancing localized corrosion [130]. The rate of degradation increases with the number of faults and defects in the parts formed. Similar to the cast alloy, the LPBF WE43 alloy displayed significantly less corrosion resistance. In r-SBF solution (revised simulated body fluid) containing fetal bovine serum up to 5%, the corrosion current density varies from 20 to 60μm/cm$^2$, and in a solution of 0.1M sodium chloride, the mass loss rate is approximately 6times greater as compared to cast WE43 alloy (0.8–1.2mm/year) [56,131]. Irrespective of higher relative density (<99%), the micro galvanic reaction attributing to high density of RE oxide and reactive magnesium matrix, resulting in the improvement in the rate of corrosion 132]. If the surface of the LPBF-WE43 scaffold is not exposed to PEO (Plasma electrolytic oxidation), it has been reported that the structural integrity of scaffold will lose after 21 days of immersion in stimulated body fluid (SBF). The research studies concluded that the corrosion resistance of the cast alloy is superior to that of the Mg-Al-based alloy. The degradation rate for AZ61 alloy formed by LPBF approach was approximately 6 to 8mm/year during the state of as-immersion, and subsequently, it decreased and gets stabilized in SBF, reducing the degradation rate to

 doi:10.20944/preprints202209.0459.v1

about 1.2 to 2.7mm/year [27]. The above-mentioned degradation is comparable to the cast AZ61 alloy in SBF depicting the rapid rise in the rate of corrosion to around 6.5mm/year, but slow down to 1.299mm/year after 24days of immersion [133-134] . The research data concluded that ZK60 alloy formed by LPBF approach provides the superior corrosion resistant as compared to cast ZK60 alloy, based on the hydrogen evolution rate and corrosion current density data [135]. Apparently, the surface of ZK60 alloy formed by LPBF approach indicate the more severe corrosion [27]. By combining ZK powders with Cu powders, Shuai et al. increased the antibacterial activity of Mg-Zn-Zr implants by adding diluted concentrations of Cu to ZK30 and ZK60 alloy formed by LPBF approach [27]. It was concluded that the LPBF ZK-Cu alloy formed by LPBF approach degrades more quickly when Cu is added. Therefore, Cu serves as the suitable alloying element to control the degradation rate of Mg-Zn-based alloy system.

2.3.3. Biocompatibility of Mg-based alloy prepared by Lased-based powder fusion

The biocompatibility of LPBF-Mg alloys must be taken into account because biodegradable implants are the most promising application for AM-Mg alloys. Being the crucial component of human body, the degradation rate of magnesium-based material shifts the stresses from implant to the rebuilt bone. Mg-based materials are equivalent to human bone in terms of both density (1.7g/cm$^3$) and Young's modulus (45GPa) [136]. Mg is both biocompatible and bioactive, which considerably encourages cellular division and proliferation [137]. The stabilization of RNA and DNA, as well as bone formation and healing, all benefit from it. Therefore, the biocompatibility of the alloying components added to the Mg-based materials attributing to the biodegradable implantation. Furthermore, the research studies depicted that the neurotoxicity of aluminum ion ($Al^{3+}$) attributing to the accumulation of these ions in the nervous system, resulting in Alzheimer's disease. Even though Al addition can increase the printability like Cu, which may have some antibacterial effects but is primarily cytotoxic [138]. Therefore, it is doubtful that alloys comprising Al and Cu will be found suitable for clinical application. Numerous research has so far confirmed the in-vitro biocompatibility of WE43 alloy formed by LPBF as a scaffold implant [56,70,139]. Although RE-based magnesium alloys themselves don't appear to have any cytotoxic potential but the extensive reactivity of the bare metal surface attributed to high evolution of hydrogen gas. The high evolution of hydrogen gas leads to the shifting of pH, which interfere with cell metabolism [27]. Only a few dead cells could be seen after direct live/dead staining, and no viable cells could be seen on the WE43 alloy formed by LPBF for scaffold applications [139]. The conclusive evidence for surface modification, such as plasma electrolytic oxidation, can address this problem since it slows the production of degradation by-products and, as a result, encourages hardly any evidence of cell damage [140]. Passivating ceramic-like surfaces also appear to provide a good option for adherent cells [141]. In addition to WE43 alloy, it was reported that the LPBF scaffold was also made using pre-alloyed system of Mg-Nd-Zn-Zr, commonly referred as JDBM [27]. Comparable to WE43 alloy formed by LPBF approach, the research study obtained by cell adhesion test identified that dicalcium phosphate dihydrate coating over the scaffold attributing to the generation of more cells that attached to scaffold rather than uncoated scaffold [27]. Neither the coated JDBM scaffold nor the uncoated JDBM scaffold formed by LPBF contributed to any significant difference in the assessment of cytotoxicity. As a result, both the samples promoted cell proliferation. From the research perspective, it was quite unacceptable that the uncoated sample of additively manufactured Mg material will not at least irritate direct cell response, hence this finding requires a more thorough investigation and verification in future.

*2.4. Challenges inherited in laser-based approach relating to Mg-based material*

The necessary manufacturing of pre-alloyed powder is difficult with regard to laser-based additive manufacturing approach. Evidence, however, points to the suitability of combining elements with a combination of pre-alloyed powders. Further research is

 doi:10.20944/preprints202209.0459.v1

needed in the area of consistency and blending of magnesium powder. To fully comprehend the physical characteristics of Mg alloys prepared by AM, mechanistic studies are still needed. Undoubtedly, laser-prepared AM alloys show distinct characteristics on comparing to non-AM Mg alloys but the physical basis resembling to such differences is still open (i.e., impact of additive manufacturing on ductility and strengthening mechanisms). While addressing to laser-based additively manufactured approach relating to Mg based material, ductility remains to be the primary concern [56]. It is recommended to have the smallest amount of powder while dealing with LPBF. But the handling and storage of powder remains to kept away from ignition, limiting the atmospheric exposure. Research finding also revealed that there exists a research gap in relation to recycling of Mg-alloy powder hasn't been investigated yet. Furthermore, compositional and process parameter modification have not yet been researched. Sintering-based approach is the new technique that needs to be explored relating to Mg-based materials. More work can be accomplished on Mg-based material by binder jetting approach. There need to look into account on post-processing approach including a homogeneous/uniform coating onto the porous scaffolds relating to Mg-alloys, that have not been investigated.

### 3. Advancement in Aluminum via Additive Manufacturing

Aluminum alloys are highly used in industrial applications due to high performance, light-weight, and low costs with good balance in between strength and density. The family of aluminum alloys are categories in various groups depending upon the heat-treated ability and primary alloy elements and shape of the alloying elements which is listed in figure. 6. In the current scenario, additive manufacturing relating to aluminum material incorporate all the industrial applications from aerospace to automotive sector. The additive manufacturing approach, SLM (Selective laser melting) can be used to produce open cell and bulk structures [142]. Aluminum alloy that is cellular or porous is a deformable, lightweight metal serving the purpose for crumple zone in automobile application [143]. Aluminum based materials that are difficult to process can be easily formed by SLM, retaining the shape benefits [142,144]. Resembling to AA-6xxx series which is difficult to produce due to its abundance of hard intermetallic, can be formed by SLM approach [145,146]. The microstructure of Al-based material i.e., cast alloy, gets refined and improved persisting to SLM approach illustrating the advantage of SLM approach [147]. In previous researches, it was obtained that the modification of microstructure attributed to the improvement in the strength of the cast Al alloys [148-151]. SLM approach offers the refinement in microstructure relating to high cooling speed in SLM without altering the chemical composition during manufacturing [145]. As a result, the requirement for the manufacture of complicated structures with precise microstructures can be satisfied by the SLM processing of castable aluminum alloys. Majorly used SLM approach is described in the below section, along with the microstructure and mechanical characteristic related to SLM approach of additive manufacturing used to prepare Al-based alloys.

Preprints (www.preprints.org) | NOT PEER-REVIEWED | Posted: 29 September 2022 doi:10.20944/preprints202209.0459.v1

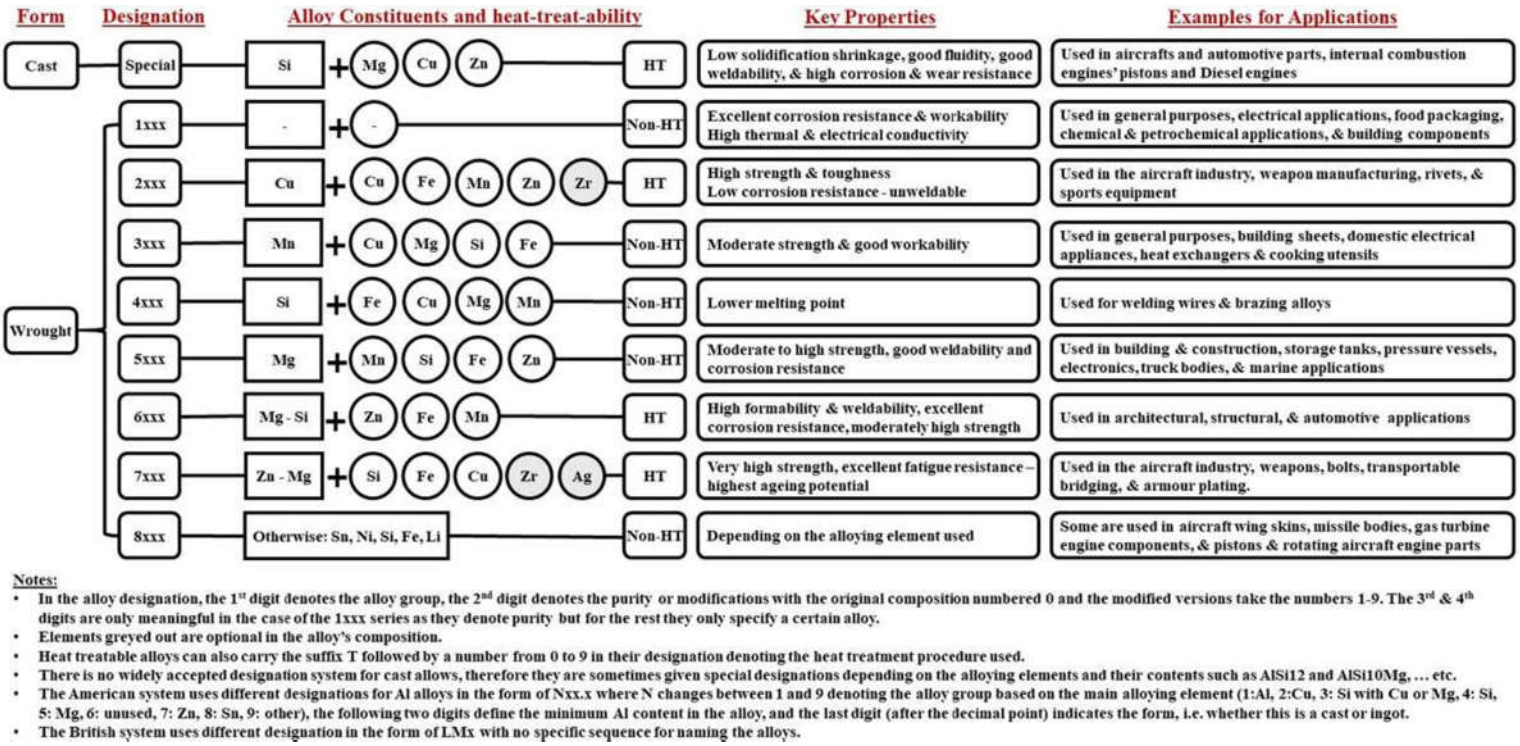


**Figure 6.** Major classification of Al alloy, highlighting the key properties and application [145].

*3.1. Selective Laser Melting approach relating to Al alloy*

Though Al-based material are difficult to processed but SLM approach providing the desired way to processed Al alloy advancing to low absorptivity of laser relating to continuous or modulated fiber lasers attributing to high thermal conductivity and reflectivity [152]. Cast alloys are often serve as the most promising aspects for SLM processing technique, indicating that AlSi10Mg and AlSi12 alloy are amongst the promising alloys [153-154]. The presence of Al-Si eutectic phase in AlSi10Mg and AlSi12 alloy attributing to excellent castability and low shrinkage, attaining the most of the attention in SLM approach. The Al-Si alloy offers high tensile characteristics and low ductility (4%) that regarded as an advantageous to Al-based material. The most frequently used high strength Al alloys used in automotive and aerospace industries are 2XXX, 6XXX, 5XXX, and 7XXX, offers increased in ductility [145-148,154]. But regardless of improved ductility and high strength, the fabrication of these above stated Al alloys is often difficult by SLM approach. The formation of micro-cracks depicted on the surface of the Al-based material formed by SLM approach due to rapid cooling persisting in processing and forming the piece attaining the low structural integrity [145,155-156]. For research perspective, the evaluation of mechanical characteristics, and microstructure of various Al alloys has been formed by laser-based additive manufacturing approach in order to illustrate the research outlook for future in SLM approach.

*3.2. Properties evaluation of Al alloy formed by SLM technique of Additive Manufacturing*

Since it is pre-requisite to analyse the mechanical characteristics of the Al-based materials in order to evaluate the viability of SLM approach that is attaining the research popularity. The microstructure refinement in the SLM approach governed by rapid solidification and material-laser interaction, attributing to the improvement in the material qualities. But simultaneously, the presence of defects adhering in the Al-based materials during the processing condition of SLM approach, attributing to negative affect on the mechanical behaviour of the Al alloy formed by SLM. Therefore, by optimizing the process parameters of SLM approach, the mechanical behaviour of Al alloy can be improved, evolving the reduction in the defects in the micro-structure of the Al-based materials. The

 doi:10.20944/preprints202209.0459.v1

variation in the processing parameters of the SLM approach influences the anisotropy of material, attributing to the different crystallographic texture of Al-based materials [145,157]. The research studies concluded that build direction had a positive affect on density of dislocations, attributing to better mechanical characteristics for AL-based SLM materials [158]. For detailed evaluation of the mechanical characteristics of laser-based Al alloy, the research studies were highlighted in the below section.

3.2.1. Nano-hardness of Laser-based additively manufactured Al alloy

The highly precise hierarchal microstructures obtained by selective-laser melting approach sparked the interest in researching the material's local mechanical characteristics at the nanoscale level [145]. The research outcomes revealed that uniform profile of melt pool in AlSi10Mg alloy at the nano-scale is obtained with depth sensing indentation approach, pertaining the improvement in the hardness of the alloy as compared to cast materials [159-161]. Resembling to the uniformity in melt pool, Everitt et al. entails that the similarity in the hardness of cast substrate, and SLM based materials, support the improvement in the hardness at the nanoscale attributed in figure. 7(a-b) [145]. The similar findings had been recognised with SiC as a reinforcement in AlSi10Mg alloy by Zhao et al. attributing to the improvement in the uniformity in nano-hardness of alloy between molten pool core and boundary [162-163]. The extremely fine microstructure and the fine dispersion of the alloying components were both credited with the uniform profile in the material formed by SLM approach [164]. In contrast, the cast material's coarser microstructure displayed spatial variation that was dependent on the indentation phase [165-166]. The researcher, Everitt et al. analysed the consistency in nano-hardness inculcating the overlapping of melt pool in the single layer, attributing to the uniformity in nano-hardness across the multi-layer sample that were showcase in Figure. 7(c-d) [161]. The research studies concluded that the researchers can infer that the local mechanical properties of the material are not significantly impacted by the overlap of the melt pools used to create the 3D structures. As, the solidification and re-melting of the material does not enhance the nano-hardness of the material irrespective grain size variation in each melt pool [167-168]. The homogeneity of the material indicated by the nano-hardness profile, depending on the melting mode up to few extents, depicted by Qi et al. studied obtaining the variation in the mechanical characteristics of AA-7050 [145]. Therefore, nano-hardness profile is regarded as the most crucial parameter in establishing the uniformity in microstructure, attributing to the improvement in the overall mechanical characteristics of the materials. As per the research studies, melting in the conduction mode attributing to the improvement in nano-hardness (higher nano-hardness), resulting in more uniformity in the hardness profile. The improvement in the area around the grain boundary with presence of fine grains relating to the increase in nano-hardness at the bottom of melt pool improves the overall mechanical characteristics of the material [169]. Figure. 7(e-f) illustrates how the local mechanical properties of the material are impacted by the microstructural changes caused by heat treatment [161]. The spheroidization of silicon and thermal treatment of the silicon particles that resulted in their coarsening caused a spatial variation in the nano-hardness of the material, with improvement in hardness being attained by the coincident indentation on silicon particle [170]. Therefore, Nano-hardness obtained by SLM approach in Al-based material is considered as an important property in order to improve the mechanical characteristics and microstructure of the material used.

Preprints (www.preprints.org) | NOT PEER-REVIEWED | Posted: 29 September 2022 doi:10.20944/preprints202209.0459.v1

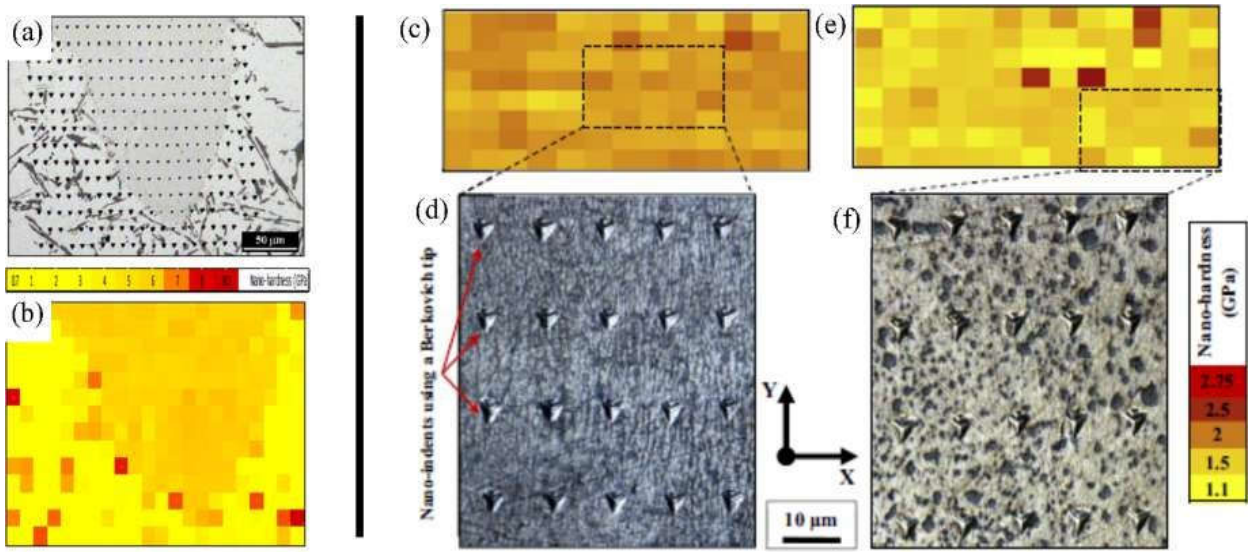


**Figure 7.** Nano-hardness image of (a) an AlSi10Mg alloy fabricated on cast AlSi12 substrate depicted (b) the homogeneity in the SLM material vs the non-uniform profile in the related part; Comparison in the nano-hardness of (c–d) the as-built material, and (e–f) the heat-treated material [161]. .

3.2.2. Micro-hardness of Laser-based additively manufactured Al alloy

Due to the relative simplicity of the test and the large number of small samples, micro-hardness is frequently used to examine the mechanical characteristics of SLM Al parts [171]. This makes it a rapid technique to evaluate mechanical characteristics, in order to widen the application filed of Al alloy formed by SLM approach. Enhanced micro-hardness for SLM AA-2XXX has been reported in comparison to its traditionally produced counterpart alloys. The as-built AA-2024 alloy has the higher value of micro-hardness ( greater than 37%) which is far more than 2024-O sheet but at the same time 20% lower as compared to T6-treated traditionally-processed sheet [145]. The major research finding up to date relating the microhardness of the Al alloy formed by SLM approach depicted in Figure 8. The variation in microhardness resembling the certain factors of SLM approach i.e., processing parameter of SLM, composition of alloying element and powder quality attributing to the variation in the densification factor. The mapping in Figure. 9 demonstrates how the material was greatly softened by the different heat treatment techniques involves solution heat treatment followed by ageing, solution heat treatment and annealing [171]. The research studies depicted the similar trends of microhardness and nanoindentation segment. The authors took into account the different alloying elements that strengthened the AlSi10Mg samples in the condition of as-built and after heat treatment [145]. The strengthening of AlSi10Mg alloy is caused by the solid solution strengthening, dislocation strengthening, and grain refinement attributing to the obstruction in the dislocation motion inherited in the material dislocations obstructing one [172]. The main difference between the as-built and heat-treated materials is that the heat treatment coarsens the grain size attributing to the formation of Si spheroids which is revealed by the Orowan strengthening criteria [173]. Inculcating the influence of the grain refinement in the microstructure, the microhardness of the as-built materials is far better than the heat-treated material. Therefore, softening of the material occurring in the process of annealing process due to the reduction in the dislocation density attributed by dislocation annihilation and coarsening of the microstructure in the heat treatment [145]. The research studies identified that AA-7075 attributed to the remarkable result by SLM approach improving the properties of the materials [145,156]. For Scalm alloy RP, the creation of a significant amount of Al3Sc prevented material softening during the T6 heat treatment, resulting in an improvement of 69% of micro-hardness [147]. Additionally, it was

Preprints (www.preprints.org) | NOT PEER-REVIEWED | Posted: 29 September 2022 doi:10.20944/preprints202209.0459.v1

claimed that Zr additions to Al alloys, either with or without Sc resulting in the similar behaviour as shown by Scalm alloy RP [174-176]. Takata et al. improvised the size of sample from 0.1mm to 10mm, in order to analyse the variation in the microhardness behaviour of AlSi10Mg alloy formed by SLM approach [177]. The study depicted that the microhardness is marginally reduced by reducing the size of sample. The obtained can be further examine in the other research studies depicting that the rate of solidification factor is directly related to the size of the sample. Therefore, the rate of solidification gets slow while reducing the size of the sample attributing to the rough microstructure, forming the softer material. The research outcomes revealed that microhardness is variable factor depending on the processing parameters, composition of alloy, powder quality and heat treatment processes.

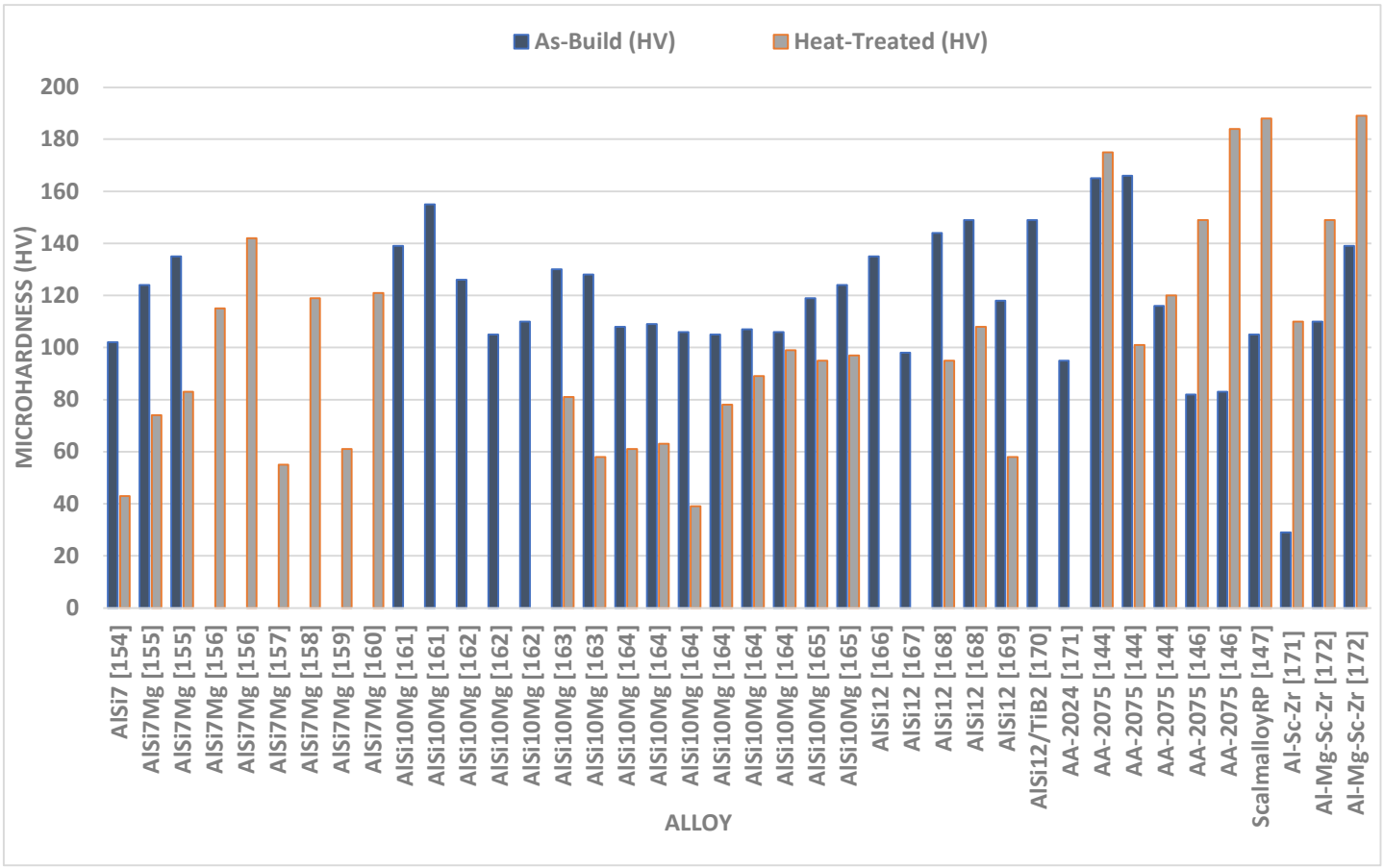


**Figure 8.** Variation in micro-hardness of Al-based materials formed by SLM approach under as-built and heat-treated condition.

Preprints (www.preprints.org) | NOT PEER-REVIEWED | Posted: 29 September 2022 doi:10.20944/preprints202209.0459.v1

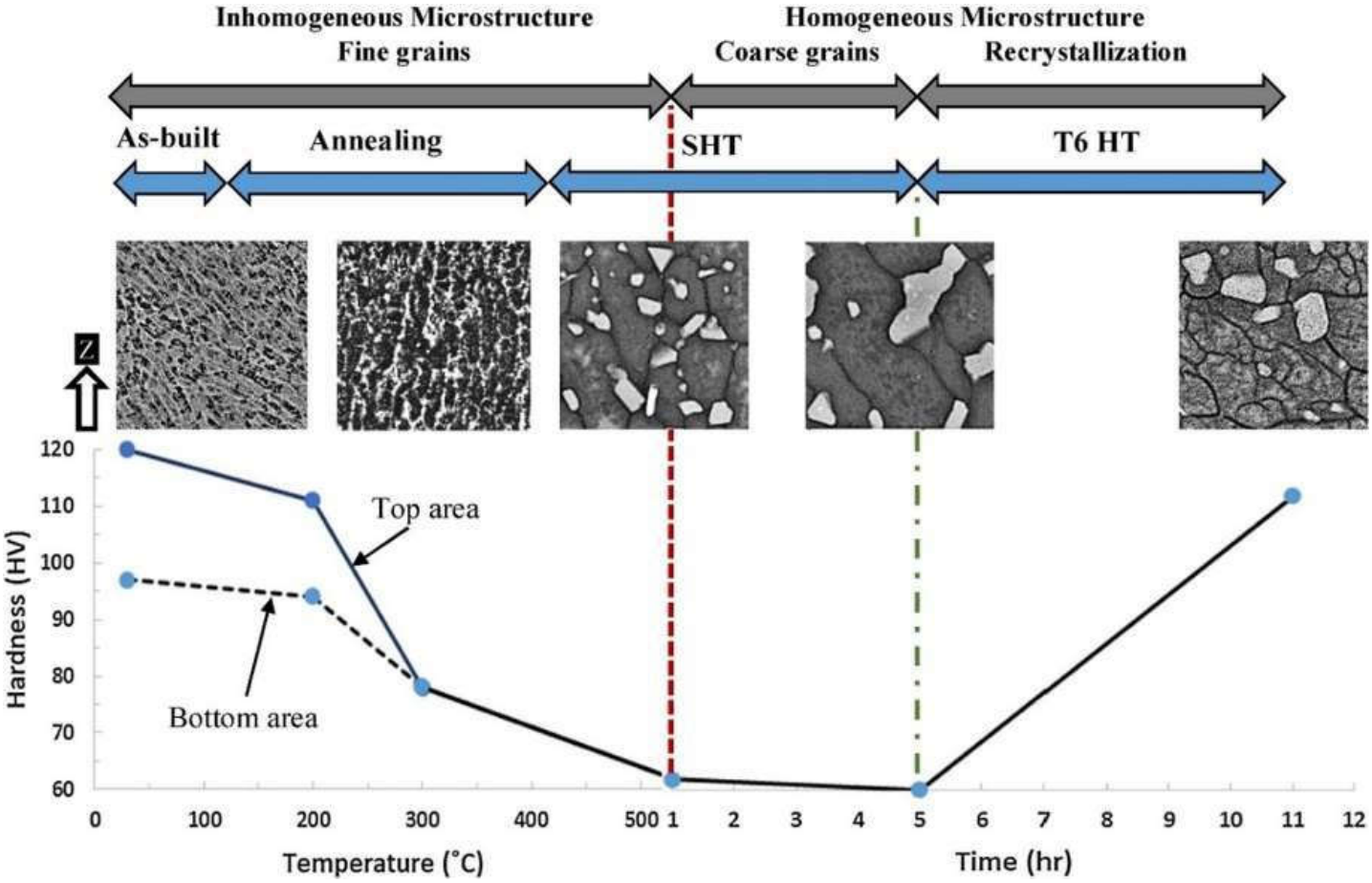


**Figure 9.** Variation in the microstructure of AlSi10Mg alloy relating the micro-hardness depending on the heat treatment process [171].

3.2.3. Tensile characteristics of Laser-based additively manufactured Al alloy

The fine microstructure of Al-based material obtained by SLM approach attributing to the improvement in the tensile strength of the material. Figure 10 illustrates the variation in the tensile characteristics of various Al alloys highlighting the research findings. The formation of sub-grain and inter-dendritic barrier evolved the improvement in the tensile strength of the Al-based materials that prevent free movement of dislocation around the boundary [145]. The AlSi12 alloy is recommended for use in applications involving high-temperature conditions due to its small drop in tensile strength and marginal improvement in ductility under elevated temperatures [119]. Micro-cracking has been demonstrated to cause poor mechanical characteristics in high-strength alloys, as reported for AA-7075 [178]. Zr nanoparticles were used to functionalize the powder's surface, which prevented cracking and improved the microstructure, giving the material tensile characteristics similar to those of wrought metal [179]. Although AA-2024's strength and ductility were better than the non-heated cast samples, they were not as good as their aged wrought counterpart. Sc-containing alloys, such as Scalm alloy RP, produced ultimate tensile strengths of more than 530MPa and elongation percentages as high as 14% as depicted in the research studies [145]. Other than that, the build orientation's anisotropy had no impact on the tensile characteristics of the Al-based materials. The evolution of precipitation of $Al_3Sc$ phase and super-saturation of Sc hinders the movement of dislocations around the boundary by pinning, attributing to the improvement in the tensile characteristics of the material [180]. The failure under tensile load surrounds the border of the molten pool when the material sample is aligned in vertical direction, depicting the detachment of the fracture from the melt pool. The coarser grains, or softer regions with

Preprints (www.preprints.org) | NOT PEER-REVIEWED | Posted: 29 September 2022 doi:10.20944/preprints202209.0459.v1

fewer grain boundaries resulting in the hindrance in the movement of dislocations [179]. The as-built specimens' finer microstructure and more homogenous dispersion of the alloying components attributing to enhancement in the tensile characteristics of the Al alloy as shown in Figure. 11(a,c). The research outcomes depicted that Si gives the material the ability to strain harden, which causes the cracks to start in the softer Al grains. As a result, the dependency of directional characteristics of Al alloy is controlled by the distribution of Si particles in the material [171]. When samples were oriented in the horizontal direction, the crack begins to propagate in the random direction spreading out in the melt pool as shown in Figure. 11(e). After heat treatment, cracks began to form and coalesce at the surface of Si particles, preferrable for the crack initiation as shown in Figure. 11(b,d). Relating to the ductility of the materials, the spherical morphology of the Si particles serves the purpose of stress concentrator that lowers the material ductility which is far superior as compared to the rod or needle like morphology in the traditionally produced material [145]. Zr was incrementally added to Al-Cu-Mg-Mn alloys to increase their tensile characteristics and ductility [181-182]. Additionally, Al-Mg alloys reinforced by Zr without Sc had exceptional tensile capabilities as a result of the development of Al3Zr precipitates (cuboidal), which were comparable to those of Sc-containing alloys without incurring the additional expense of adding Sc [145]. Al3Zr precipitates at nano- and submicron sizes helped to refine the grain, avoiding hot tearing in solidification process and boosting strength via the Hall-Petch effect. In addition, the material has a far higher toughness than the alloys that contain Sc [187]. Resembling to the low laser absorptivity of the consolidated metal, a shallower melt pool that were formed during the second scan enabled further refining. The research studies revealed that Zr-modified alloy had evolved the higher ductility than the Sc-modified alloys. Changing the chemical composition of the Al-Si alloys is another way to significantly strengthen them while still utilising SLM's relative processing simplicity, as demonstrated by Pozdniakov et al. [145]. This alloy provided a compromise between strength and ductility through heat treatments.

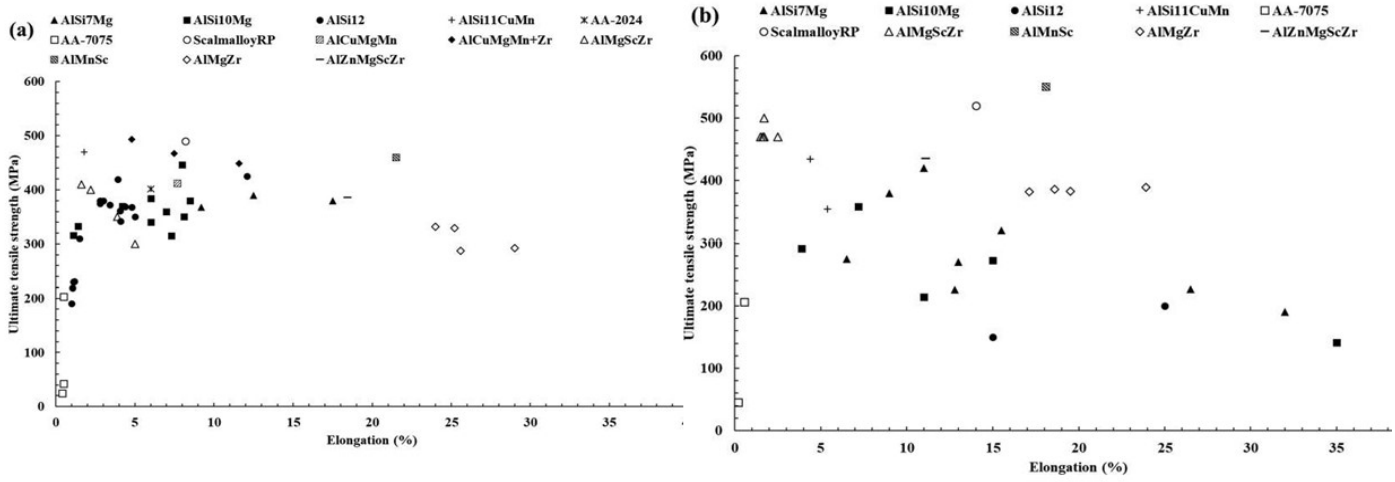


**Figure 10.** Variation in the Tensile strength vs elongation (%) for Al-based material formed by SLM approach in as-built and heat-treated condition [145].

Preprints (www.preprints.org) | NOT PEER-REVIEWED | Posted: 29 September 2022 doi:10.20944/preprints202209.0459.v1

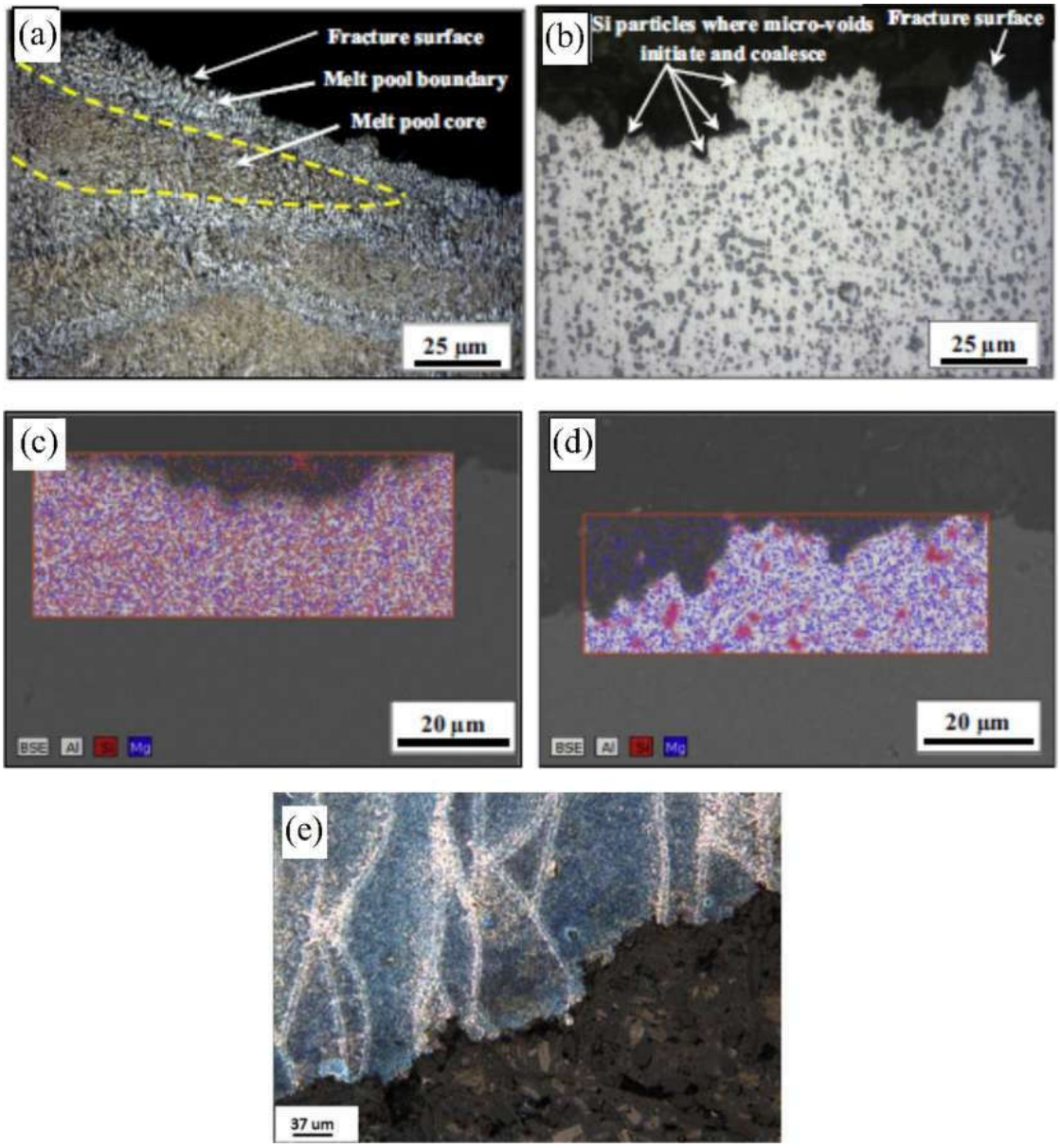


**Figure 11.** Tensile fracture of AlSi10Mg alloy formed by SLM approach oriented cross-sectionally comparing (a) as-built sample in the horizontal direction with EDS mapping (c), the heat-treated specimen (b) and (d). The fracture surface of an as-SLM specimen oriented in the horizontal direction (e) [161,187].

### 3.2.4. Compressive Characteristics of Laser-based additively manufactured Al alloy

Despite the improvement brought about by heat treatment, the compressive characteristics of the high-strength alloy AA-7075 was obtained to be inferior as compared to the conventional counterpart. It's important to remember that this finding applied to AA-7075 with the addition of 4% Si particles attributing to the lessen cracking. Inability to restrict the propagation of cracks can lead to poor performance of AA-7075 alloy [145]. The compressive strength of an AlMg6.5 alloy with Sc and Zr additions was improved, and the results varied with the energy density [184]. The greater compressive strength (1.08GPa) of the Al85Nd8Ni5Co2 alloy was maintained even at the higher temperature corresponds to heat treatment [185]. The creation of a composite-like material after the SLM process in the form of an Al matrix supplemented with $AlNd_3$, $Al4CoNi_2$, and $AlNdNi_4$; these reinforcements induced fracture deflection under stress [145]. Additionally, the distinctive microstructure produced compressive behaviour that was superior to the counterpart that had undergone normal processing [185]. AlSi10Mg was reported to have a compressive

 doi:10.20944/preprints202209.0459.v1

yield strength three times greater than the cast material [145]. An AlSi12-TNM composite that displayed increased compressive characteristics at the cost of flexibility attributing that the usage of reinforcement increased the compressive strength of the alloy [145]. $TiB_2$ particles were added to AlSi12 to increase its compressive strength while maintaining the material's ductility by removing its crystallographic texture [187]. Although the compressive behaviour of Al-based materials has not previously garnered much attention, it is now becoming more significant since aluminum alloys are utilised more frequently in lattice structures made by SLM, where compressive strength is the most critical mechanical characteristics. Overall, the research findings concluded that SLM-fabricated components have better compressive performance than conventionally-processed parts make them appealing for a variety of applications.

3.2.5. Fatigue characteristics of laser-based additively manufactured Al alloy

SLM materials typically perform less well in terms of fatigue than their conventionally made counterparts. This has been linked to a number of causes in the literature, including the fact that second phase particles in cast alloys make fatigue performance vulnerable to common SLM flaws including porosity, residual stresses, and surface roughness [145]. These serve as stress concentrations that shorten fatigue life by causing cracks to form and spread. The S-N curves from several studies are displayed in Figure 12, which contrasts the performance of the conventionally-cast material with the acceptable fatigue strength observed in SLM components made of Al alloys due to the finer microstructure created in the material [156]. A large difference in fatigue characteristics results from the variability between parts made from various powders on various systems utilising a wide range of process settings. SLM parts made of alloys like AlSi10Mg and Al6061, among others, have been reported to include internal pores harbouring unbonded powder [161]. They may not significantly diminish the load carrying area under tension while being relatively small, but during cyclic loading, they may have a more noticeable impact. The fatigue life is reduced as the flaw size increases [174]. Additionally, oxides that develop at these holes or are randomly distributed across the samples cause early failure. These oxides and holes are frequently seen where cracks first appear as depicted in figure. 13(a-f). These oxides are thought to arise as a result of laser spatter, oxidized vapour, and the original oxide layer on the powder utilised in the process [188]. Supporting structures are added to sections with overhangs to increase the cooling rate, which forces the creation of a finer microstructure and increases the material's fatigue strength. Brandl et al. observed that the build-plate temperature does not impact the fatigue strength of SLM AlSi10Mg but rather lowers data scatter [189]. The scatter in the results for AlSi12 was also decreased by heating the build-plate. The improvement in fatigue strength contradicted a previous finding by Siddique et al. illustrated in figure 12(b). It's unclear what caused this difference. Several techniques, including sandblasting, shot peening, rolling, burnishing, heat treatments, and hot isostatic pressing, can increase the fatigue life of parts. AlSi10Mg's fatigue strength was increased through shot peening employing steel and ceramic balls, outperforming samples that had undergone conventional processing as depicted in Figure 12(c). According to Brandl et al. and Aboulkhair et al., a typical T6 heat treatment significantly increased performance, which is illustrated in Figure 12(d) by softening the material and therefore enhancing ductility [145]. The component is also vulnerable to premature failure when subjected to cyclic loads due to surface open pores or sub-surface porosity. A ring of porosity at the sample's surface was seen by Damon et al. [145]. In the author's work, it has been shown that milling, which is typically done to increase the surface roughness of SLM samples, causes sub-surface pores to come to the surface and increases data scatter. These pores were discovered to be the locations where cracks begin, spread, and ultimately fail. Yang et al. compared samples with machined surfaces that still had some sub-surface porosity to samples that allegedly had none. Both of them outlasted the life of the as-built samples, but the latter demonstrated a better fatigue life [176]. As a result, the sub-surface pores have a negative impact on the SLM samples' fatigue life.

Preprints (www.preprints.org) | NOT PEER-REVIEWED | Posted: 29 September 2022 doi:10.20944/preprints202209.0459.v1

Siddique et al. suggested repeatedly checking the shapes of the pieces for re-melting to lessen the likelihood of porosity development in these areas. Due to the direct relationship between a material's ductility and fatigue strength, several process variables, such as build orientation and build-plate temperature, also have an impact on fatigue performance [121]. This was also anticipated for the material's fatigue resistance, given that the ductility of the SLM material demonstrated signs of anisotropy dependent on the build orientation. The samples constructed in a horizontal position have a longer fatigue life than samples constructed in a vertical configuration.

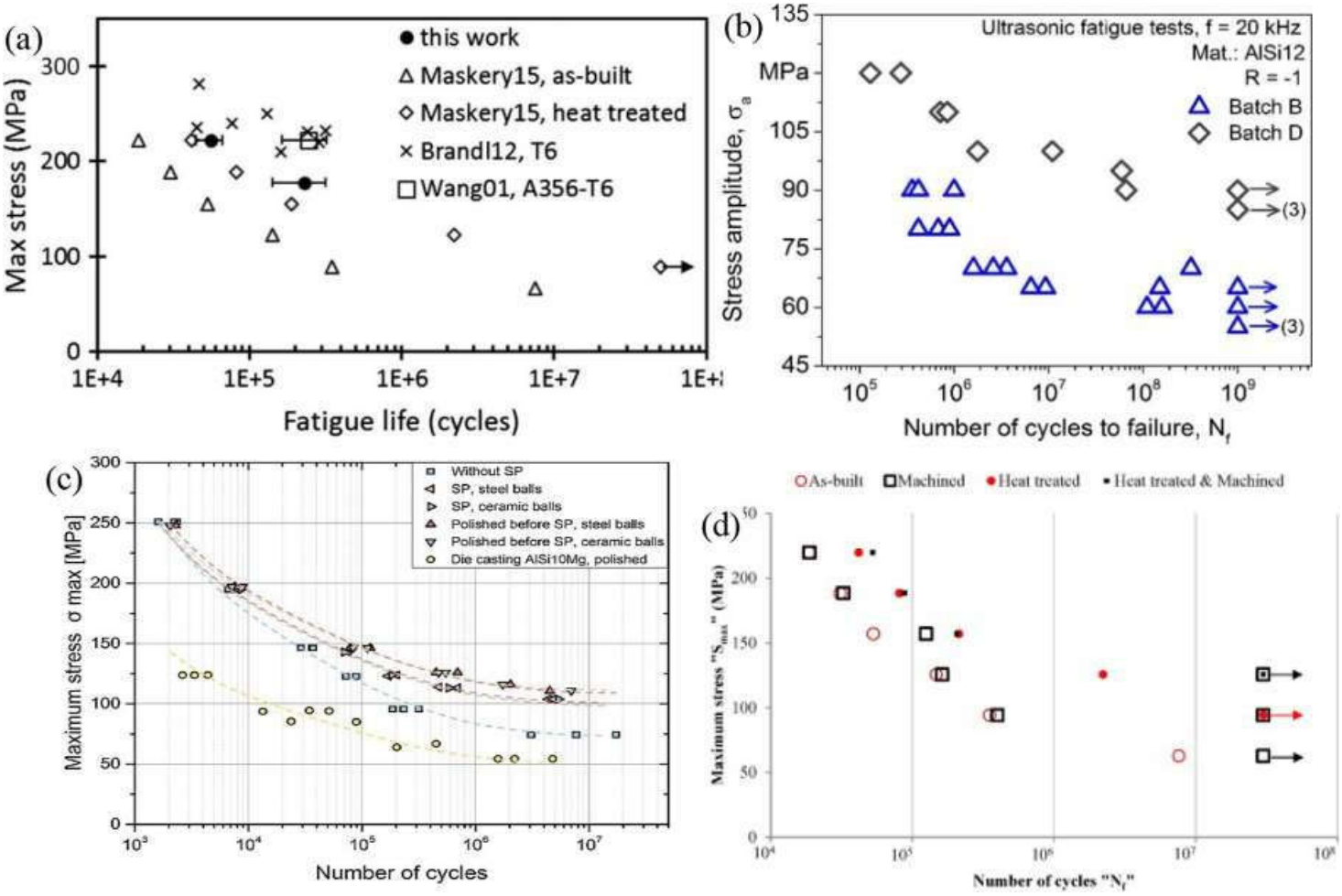


**Figure 12.** (a) fatigue characteristics for AlSi10Mg alloy formed by SLM approach, (b) S-N curves for AlSi12 alloy formed by SLM approach revealing the effect of build plate heating, where batch B is does not involved build plate temperature while batch D involved build plate temperature of 200 °C, (c) S-N curves revealed shot peening of AlSi10Mg alloy sample, (d) S-N curves AlSi10Mg alloy revealed variation in fatigue characteristics corresponds to machining of material and heat treatment [190-192].

Preprints (www.preprints.org) | NOT PEER-REVIEWED | Posted: 29 September 2022 doi:10.20944/preprints202209.0459.v1

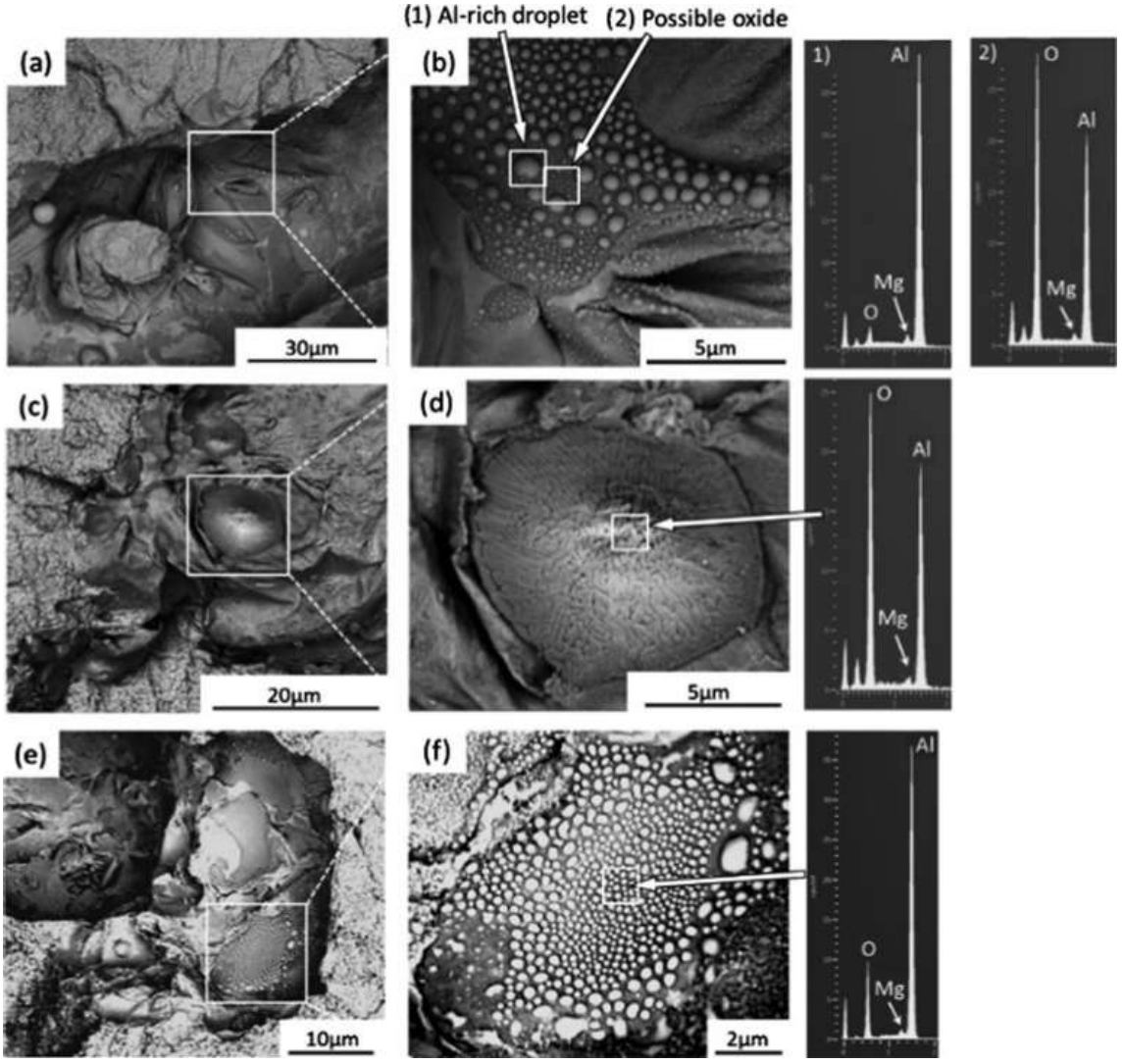


**Figure 13.** Formation of oxides in the SLM sample at the crack initiation region [193].

3.2.5. Fracture and creep characteristics of laser-based additively manufactured Al alloy

The ability of a material to withstand crack propagation is determined by its fracture toughness. The ductility of a substance directly relates to its toughness. Despite having less ductility, the SLM material's toughness significantly outperformed that of the cast material by a factor of almost three or four. This is caused by the interdendritic Si that is present at the Al cell borders and prevents the crack from spreading [145]. Additionally, the crack is forced to alter its course rather frequently as a result of the circular topology of the melt pools and the preferred crack propagation at their boundaries, which results in increased fracture toughness. As a result, samples formed in different build orientations have different fracture toughness with vertical samples having the lowest fracture toughness due to the anisotropic microstructure produced by SLM [165-174]. Annealing decreased the material's fracture toughness even while its ductility and strength increased. The lower resistance to crack propagation, or poorer fracture toughness, is thought to be caused by the structural disintegration of the melt pool boundary. The heat-treated material was still twice as tough as its cast equivalent, though. SLM provides the opportunity to fabricate parts that simultaneously benefit from increased strength and ductility [20, 40-45,145]. This advantageous mix of features cannot be obtained by utilising standard processing methods. The evaluation of a material's time-dependent mechanical performance at high temperatures is called creep resistance. It depends on the material at what temperature creep becomes a design issue [145]. Al is understood to creep at temperatures

 doi:10.20944/preprints202209.0459.v1

between 200 and 300 °C because it has a comparatively low melting point [194]. According to Read et al., the creep resistance of SLM AlSi10Mg components is in line with expectations for this material, i.e., comparable to the material that has undergone conventional processing [195]. The creep resistance decreased as testing temperature or load/stress increased, as was to be predicted. At higher temperatures, recovery can begin, which causes creep resistance to degrade. Increasing the barriers that restrict the dislocation motion is one strategy for increasing creep resistance [145, 174, 195]. The research studies depicted that the high dislocation density of Al alloy formed by SLM approach attributing to the improvement in the creep resistance of the alloy. It is anticipated that these dislocations will entangle and function as barriers to one another, increasing the resistance to deformation. In contrast to the tensile characteristics, creep resistance is typically improved for materials with bigger grain sizes. This is because the higher grain size reduces the diffusion rate and restricts the sliding of grain borders, two factors that are crucial for creep. For age-hardenable Al alloys, the presence of precipitates in the material also increases creep resistance [196].

3.2.6. Impact and Wear resistance laser-based additively manufactured Al alloy

Analysing the impact resistance behaviour is likely more pertinent for lattice structures in the SLM sector. This is caused by their potential for usage in energy absorption applications and as an impact-protective mechanism. The most common method of evaluating a material's impact resistance is to experimentally measure the impact energy, or the effort required to shatter a specimen. After impact, the sample absorbs the energy up to the yield point, at which point plastic deformation begins [140-145]. The material breaks as it hits the limit and is no longer able to absorb additional energy. The complex dynamic behaviour of the material can be controlled by regulating the struggle strain hardening developed in the material (to peak flow stress) following by thermal softening. SLM parts outperformed their traditionally processed counterparts in terms of impact resistance, just like the other sorts of mechanical strengths that have been discussed up to this point [190]. Although this was not anticipated because poor impact resistance often goes hand in hand with low ductility. As-processed SLM samples from Charpy impact testing had impact energies that were either on par with or superior to (by about 1.5 times) the cast material. The dynamic yield strength of heat-treated samples from planar impact testing was nearly twice as high as the dynamic tensile strength of the sand-cast counterpart [176]. The finer, more homogenous microstructure is what gives the material its increased impact strength. Impact resistance was not affected by anisotropy, despite it having considerable influence on some mechanical parameters (the material's resistance to impact was independent of the build orientation) [197].

For advancement in the automobile sector where a part may undergo a large degree of friction in application, the tribological behaviour of an SLM Al part is very crucial [145,198]. In the family of Al-Si alloys, the wear resistance of the material increases with increasing Si concentration [191]. SLM's finer grain structure, which outperforms that of its cast and extruded counterparts, results in high resistance to wear in the sliding wear condition. For wear caused by corrosion and erosive processes, similar outcomes were seen [199-200]. The materials can be strengthened to increase their wear resistance [145]. In comparison to ceramic reinforcements, metallic reinforcements offer superior compatibility with the parent metal. The SLM process settings have an impact on the wear mechanism, which is primarily abrasive for higher hardness materials and shifts to adhesive as the hardness declines. The hardness of a substance directly relates to how resistant it is to wear. As a result, parts in their as-built condition show the lowest wear rate, whereas annealing softens the material and increases wear rate as shown in Figure 14(a). Figure 14(b) compares the SLM material's tribological behaviour to that of its cast equivalent [201-202]. The greater tribological behaviour is warranted because SLM procedures result in material that is tougher than what is produced by conventional processes. The presence of a surface oxide layer, which is eliminated during the initial rounds of sliding in a wear

Preprints (www.preprints.org) | NOT PEER-REVIEWED | Posted: 29 September 2022 doi:10.20944/preprints202209.0459.v1

test, causes the coefficient of friction in SLM samples to be greater at the surface [203]. Beyond this layer, the coefficient of friction stabilises and starts to more accurately reflect the capabilities of the material. This was attributed by Kang et al. to the weld-fracture process that was prevalent in soft metals prior to stabilisation [145]. Variations in the coefficient of friction patterns are one way that this is seen. The softer the material, the longer the fluctuation region [204-205]. Due of the limited weld-fraction process, samples with substantial porosity typically don't exhibit any fluctuation region.

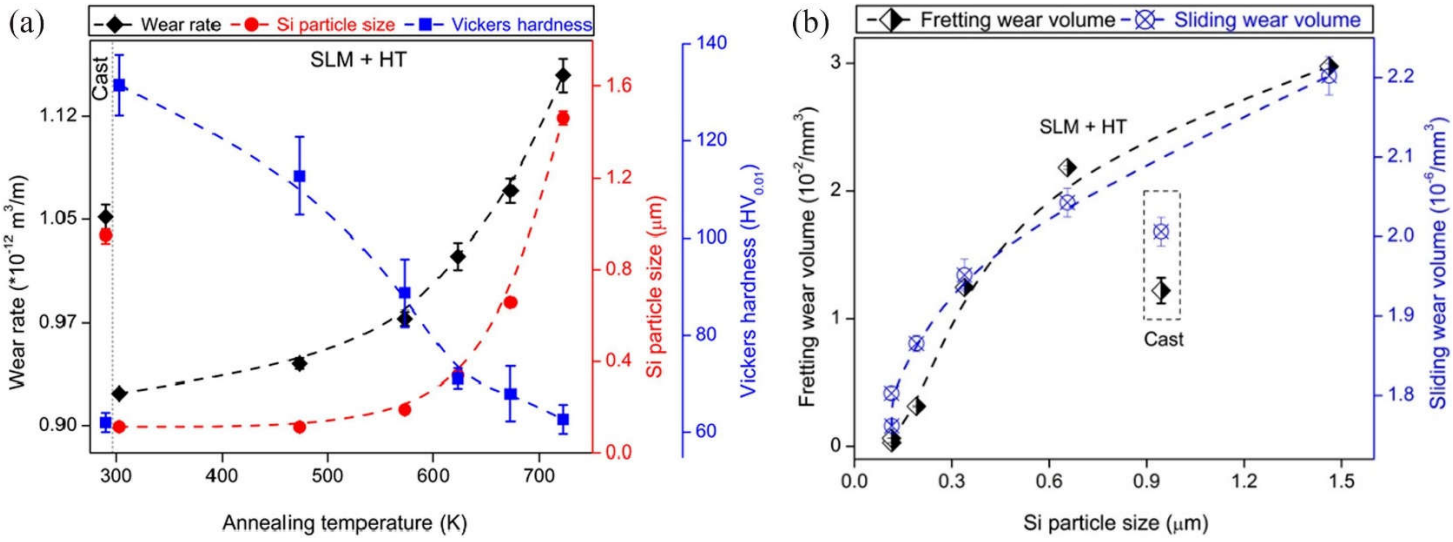


**Figure 14.** (a) Influence of heat treatment process on the hardness and wear of AlSi12 alloy formed by SLM approach, (b) tribological behaviour of the materials formed by SLM approach comparable to cast counterpart [145].

### *3.3. Metallurgy of laser-based additively manufactured Al alloy*

#### 3.3.1 Microstructure of Al alloy formed by SLM

The creation of the microstructure is governed by the temperature during SLM. During processing, the material is exposed to directional heat transfer and significant thermal gradients [145]. It is also repeatedly remelted as a result of internal heat transfer and the laser beam's ability to pass through layers. With increasing laser power and scan speed, solidification happens at an incredibly fast pace (103–108 K/s), resulting in a thin microstructure with metastable phases [156]. As an alternative to the coarse microstructures created by normal manufacturing, this fine microstructure is in demand. In Figure 15, a comparison of the microstructures created by casting and SLM is shown. The microstructure outlined above was discovered to be in conformity with the sequence provided by the AlSi10Mg phase diagram estimated using Calphad by Takata et al. [201]. They also noted that the size of the generated sample affected the microstructure of the material created. Si particles were found inside the columnar Al grains of smaller samples, ranging in size from 0.1 to 0.3 mm, demonstrating that Si precipitated during SLM under these circumstances [145]. The effectiveness of the heat flow can be used to explain this. When compared to the solidified material surrounding the melt pool in the case of the bigger samples, the melt pool in the smaller samples is surrounded by unmolten powder, which has a reduced heat conductivity. Due to the comparatively modest rate of solidification imposed by the decreased thermal conductivity and the lengthy periods of increased temperatures, Si can precipitate in the columnar Al grains [206]. Figure 16 depicted the microstructure of SLM AlSi10Mg in isometric views for as-built and (b) after heat treatment. Figure 17 entails the EBSD image of AlSi10Mg grain structure produced by SLM with columnar cells growing perpendicular to the build direction, and SEM images show the microstructure in the dashed region and the grain structure using a secondary electron detector and a backscatter electron detector [207].

Preprints (www.preprints.org) | NOT PEER-REVIEWED | Posted: 29 September 2022 doi:10.20944/preprints202209.0459.v1

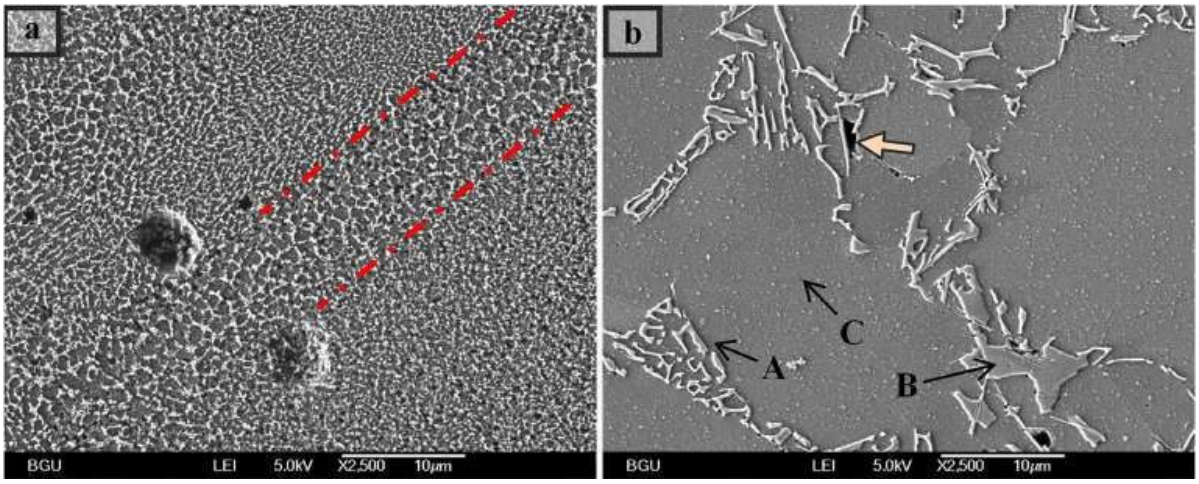


**Figure 15.** SEM image depicted AlSi10Mg microstructure formed by (a) SLM, (b) casting. The arrows in (b) pointing to (A) Al-Si eutectic, (B) Si dispersed in Al matrix, and (C) Fe-containing intermetallic phases [191].

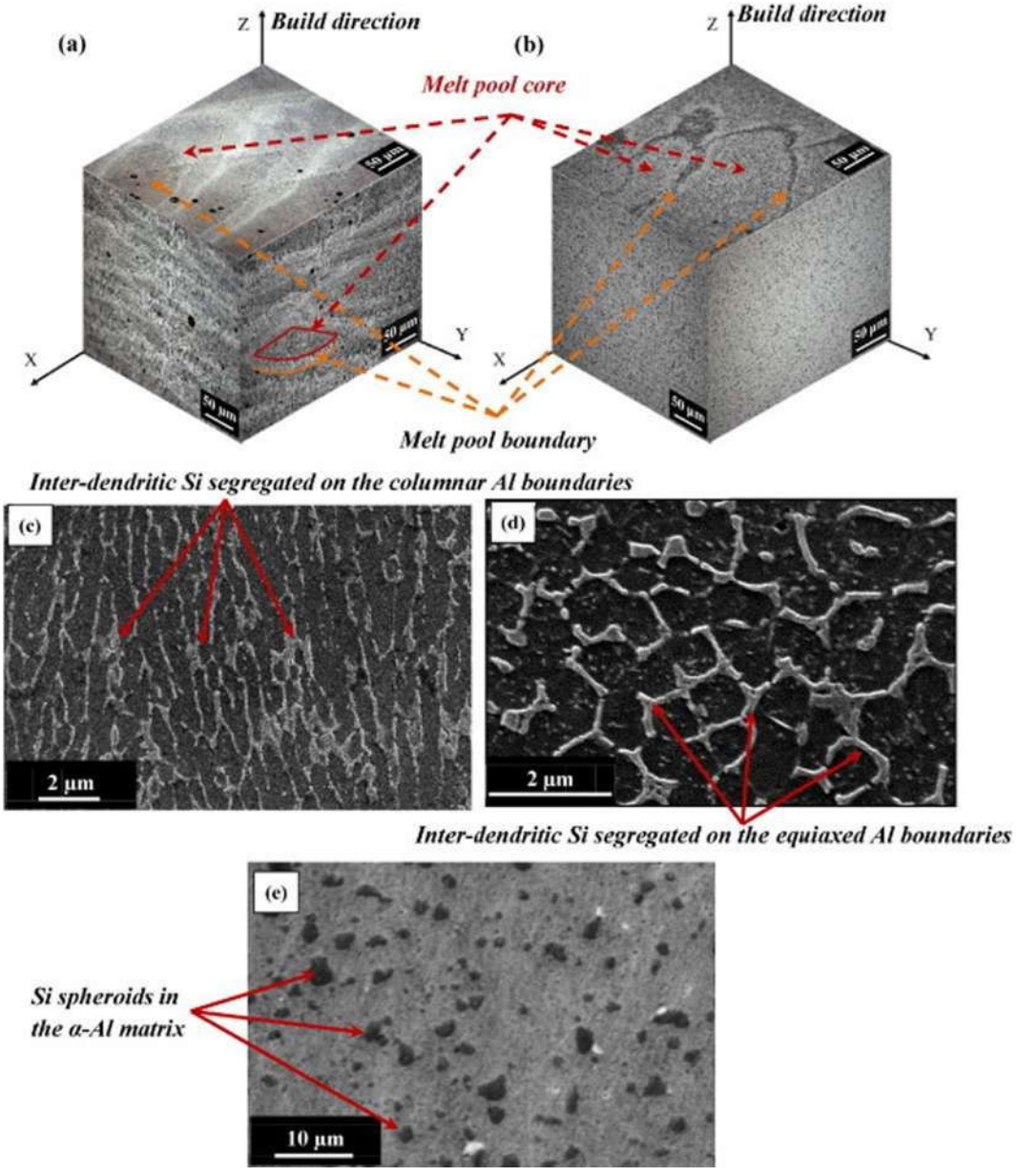

Preprints (www.preprints.org) | NOT PEER-REVIEWED | Posted: 29 September 2022 doi:10.20944/preprints202209.0459.v1

**Figure 16.** The microstructure of SLM AlSi10Mg is shown in isometric views in the following order: (a) as-built, (b) after heat treatment; (c-d) elongated $\alpha$ -Al and equiaxed $\alpha$ -Al grains as seen on the XY plane in the as-built material and (e) Si spheroids in the $\alpha$ -Al matrix after T6 heat treatment [192].

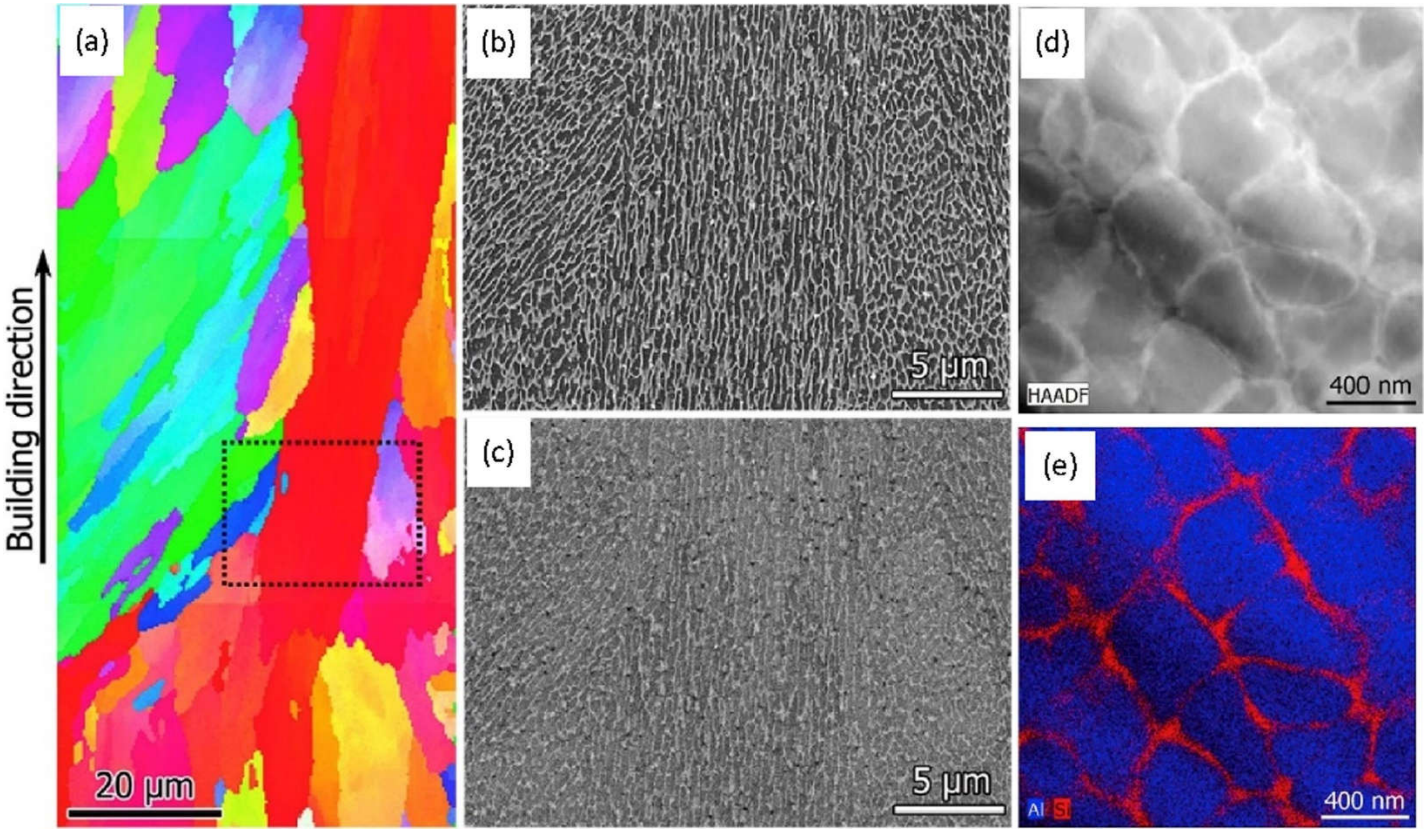


**Figure 17.** The (a) EBSD image depicts the AlSi10Mg alloy grain structure obtained by SLM with columnar cells developing perpendicular to the build direction, (b-c) SEM images show the microstructure in the dashed region and the grain structure using a secondary electron detector and a backscatter electron detector, respectively. As-built SLM AlSi10Mg cells' STEM images and associated Al-Si EDX maps are displayed in (d-e) [207].

### 3.3.2. Crystallographic texture of laser-based additvely manufactured Al alloy

Despite the lack of mechanical processing necessary for deformation texture in SLM, temperature gradients and rapid cooling rates encourage the epitaxial development of columnar grains in the majority of Al alloys. This texture results in mechanical anisotropy, crack susceptibility, and yield strength and elongation at failure. The directional solidification within the melt pool is the source of the crystallographic texture found in SLM Al components [145]. However, the selection of processing settings and the thermo-physical characteristics of the material have a considerable impact on the geometry of the melt pool, which in turn affects the heat flow direction at the liquid/solid boundary and the pace of solidification [176]. As a result, depending on the tools and feedstocks employed, the strength of the final grain texture varies greatly. The average grain growth direction during the initial phases of melt pool solidification depends on the solidification front direction (usually perpendicular to the melt pool boundary) and thermal gradients. Due to constitutional undercooling being prevented in the majority of Al alloys due to high thermal conductivity and solidification velocities, thermal gradients are primarily in the opposite direction of the build direction, or radial, depending on the melt pool width-to-depth ratio [145]. These circumstances produce morphological grain texture, with elongated grain structures emerging from the melt pool boundaries in the longitudinal cross-section of SLM components. Numerous researches have in fact proven the relationship between the morphological and

 doi:10.20944/preprints202209.0459.v1

crystallographic textures of the grain created by the melt pool boundary. According to Wu et al., elongated grains of SLM AlSi10Mg (discovered close to melt pool boundaries) are made up of sub-cells with the same orientation. According to Thijs et al. [140], this dominant grain orientation results in a fiber texture component with a {1 0 0} along the scan direction depicted in Figure 18. Figure 18 also depicted the Inverse pole figure orientation map displaying the elongated grain structure's predominately {1 0 0} orientation along the build direction. Additionally, the orientation map reveals a finer grain structure at the melt's sides and top, but there is no clear dominating orientation [208]. Suryawanshi et al. reported similar outcomes for AlSi12 as well. The elongated grain structure of AlSi10Mg and Al-Mg-Cu, on the other hand, has a dominant {1 0 0} texture along the build direction, as shown by Takata et al. and Zhang et al. [208-214]. These variances are attributed to variations in the melt pool shape geometry and consequently thermal gradients, while not being stated directly. Elongated grains either consume the residual liquid when the melt pool solidifies or a refined equiaxed grain structure develops [156]. Equiaxed grains are those that have no prominent crystallographic texture and are desired to minimize mechanical anisotropy. They are anticipated to form in alloys with narrow solidification ranges from surface nucleation. Recent studies have concentrated on methods to create a melt pool with a more refined, homogeneous structure that would eliminate any crystallographic roughness and lessen solidification cracking. It has been proven successful in promoting refined texture-free melt pool grain structures in a number of Al alloys, including Al-Mg-Zr, AA-2XXX, AA-6061, and AA-7075, by adding suitable heterogeneous elements that increase the density of nucleation sites in the melt pool and encourage columnar to the equiaxed transition of the grain structure [145].

Preprints (www.preprints.org) | NOT PEER-REVIEWED | Posted: 29 September 2022 doi:10.20944/preprints202209.0459.v1

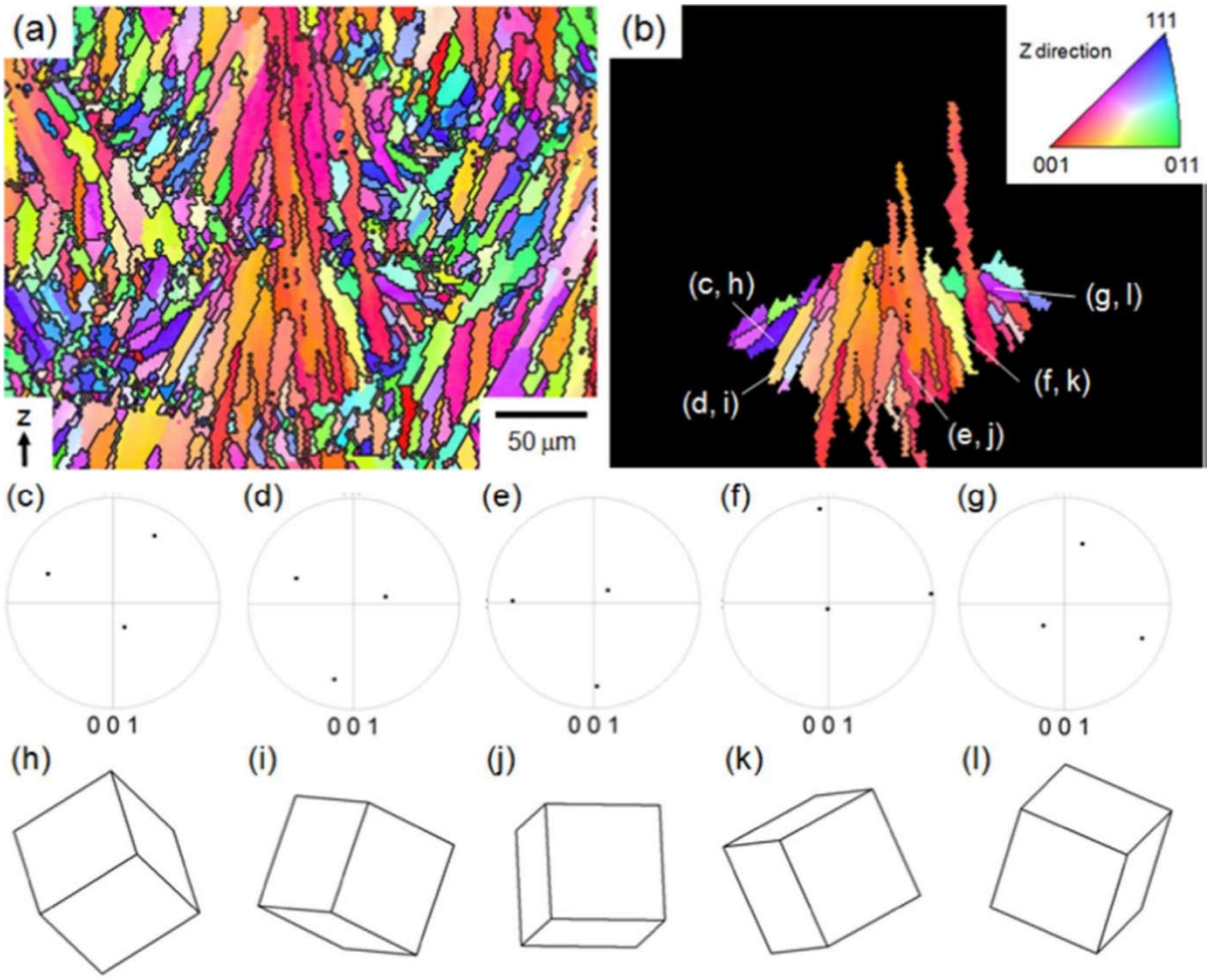


**Figure 18.** Inverse pole figure orientation map displaying the elongated grain structure's predominately {1 0 0}orientation along the build direction. Additionally, the orientation map reveals a finer grain structure at the melt's sides and top, but there is no clear dominating orientation [208,211].

## 4. Conclusion and Future Prospect

The work-study successfully examines the advancement of magnesium and aluminum alloy in the role of additive manufacturing. The laser-based additive manufacturing approach is a quite useful technique used for as-cast and heat-treated magnesium and aluminum alloy. The investigation of various aluminum and magnesium alloy is successfully accomplished. The influence of laser-based additive manufacturing on the mechanical characteristics of magnesium and aluminum alloy is examined. The advancement of additive manufacturing in building the light-weight material (magnesium and aluminum material) has been reviewed. The investigation of novel magnesium alloys has a lot of potential. components that are incredibly light and use empty space as a design factor. As with any new development in this environment, it would broaden the usage base as the qualities of the materials change to meet the needs of new markets. New smart device and components for biomedical applications can be suitably be formed using LBPF approach of additive manufacturing for Mg-based alloys. Today, a sizable amount of work is being done in the area of SLM of Al alloys. To focus future research on areas that can raise the status of the technology, some restraint is required. There is currently a dearth of research into how the sample size affects the choice of process parameters. It has not yet been thoroughly investigated how these process parameters translate to the manufacturing of noticeably small features, such as in the case of lattice systems. Custom scan-strategies for lattice

 doi:10.20944/preprints202209.0459.v1

structures can raise their performance by raising their quality. Two paths have been taken in research to address the flaws in SLM parts: in-process or post-processing. Higher build-plate temperatures have the ability to reduce the flaws formed throughout the process, but they may have an adverse influence on the material's microstructure, mechanical characteristics, and process efficiency. For the process to achieve its demands by creating powder with specifications meeting the process criteria, it is crucial to standardise the qualities of metal powders for SLM. Despite the fact that powders that don't completely meet the standards for the process can still be used to produce parts without any defects. To fully utilise this potential, high-throughput methods to experimentally evaluate the bespoke alloys and materials design software are required. Understanding how the alloying components affect the material's capacity to be processed by SLM and, eventually, the qualities of the manufactured parts in use.

**References**


1. Huang, Y., Leu, M. C., Mazumder, J., & Donmez, A. (2015). Additive manufacturing: current state, future potential, gaps and needs, and recommendations. Journal of Manufacturing Science and Engineering, 137(1).
2. Dilberoglu, U. M., Gharehpapagh, B., Yaman, U., & Dolen, M. (2017). The role of additive manufacturing in the era of industry 4.0. Procedia Manufacturing, 11, 545-554.
3. Posten, C., & Schaub, G. (2009). Microalgae and terrestrial biomass as source for fuels—a process view. Journal of biotechnology, 142(1), 64-69.
4. Posten, C., & Schaub, G. (2009). Microalgae and terrestrial biomass as source for fuels—a process view. Journal of biotechnology, 142(1), 64-69.
5. Stock, T., Obenaus, M., Kunz, S., & Kohl, H. (2018). Industry 4.0 as enabler for a sustainable development: A qualitative assessment of its ecological and social potential. Process Safety and Environmental Protection, 118, 254-267.
6. Ford, S., & Despeisse, M. (2016). Additive manufacturing and sustainability: an exploratory study of the advantages and challenges. Journal of cleaner Production, 137, 1573-1587.
7. Aboulkhair, N. T., Simonelli, M., Parry, L., Ashcroft, I., Tuck, C., & Hague, R. (2019). 3D printing of Aluminium alloys: Additive Manufacturing of Aluminium alloys using selective laser melting. Progress in materials science, 106, 100578.
8. Weng, W., Biesiekierski, A., Li, Y., Dargusch, M., & Wen, C. (2021). A review of the physiological impact of rare earth elements and their uses in biomedical Mg alloys. Acta Biomaterialia, 130, 80-97.
9. Echeverry-Rendon, M., Allain, J. P., Robledo, S. M., Echeverria, F., & Harmsen, M. C. (2019). Coatings for biodegradable magnesium-based supports for therapy of vascular disease: A general view. Materials Science and Engineering: C, 102, 150-163.
10. Wu, Shuilin, Xiangmei Liu, Kelvin WK Yeung, Changsheng Liu, and Xianjin Yang. "Biomimetic porous scaffolds for bone tissue engineering." Materials Science and Engineering: R: Reports 80 (2014): 1-36.
11. Liu, Shiyang, Damon Kent, Nghiem Doan, Matthew Dargusch, and Gui Wang. "Effects of deformation twinning on the mechanical properties of biodegradable Zn-Mg alloys." Bioactive Materials 4 (2019): 8-16.
12. Zeng, Zhuoran, Nicole Stanford, Christopher Huw John Davies, Jian-Feng Nie, and Nick Birbilis. "Magnesium extrusion alloys: a review of developments and prospects." International Materials Reviews 64(1), (2019): 27-62.
13. Childerhouse, Thomas, and Martin Jackson. "Near net shape manufacture of titanium alloy components from powder and wire: A review of state-of-the-art process routes." Metals 9, no. 6 (2019): 689.
14. Horn, Timothy J., and Ola LA Harrysson. "Overview of current additive manufacturing technologies and selected applications." Science progress 95(3) (2012): 255-282.

15. Attaran, M. (2017). The rise of 3-D printing: The advantages of additive manufacturing over traditional manufacturing. Business horizons, 60(5), 677-688.
16. Gibson, Ian, David W. Rosen, Brent Stucker, Mahyar Khorasani, David Rosen, Brent Stucker, and Mahyar Khorasani. Additive manufacturing technologies. Vol. 17. Cham, Switzerland: Springer, 2021.
17. Qin, Yu, Peng Wen, Hui Guo, Dandan Xia, Yufeng Zheng, Lucas Jauer, Reinhart Poprawe, Maximilian Voshage, and Johannes Henrich Schleifenbaum. "Additive manufacturing of biodegradable metals: Current research status and future perspectives." Acta biomaterialia 98 (2019): 3-22.
18. Vanmeensel, Kim, Karel Lietaert, Bey Vrancken, Sasan Dadbakhsh, Xiaopeng Li, Jean-Pierre Kruth, Pavel Krakhmalev, Igor Yadroitsev, and Jan Van Humbeeck. "Additively manufactured metals for medical applications." Additive manufacturing (2018): 261-309.
19. Singh, Shweta, and Naresh Bhatnagar. "A survey of fabrication and application of metallic foams (1925–2017)." Journal of Porous Materials 25, no. 2 (2018): 537-554.
20. Kayode, O., & Akinlabi, E. T. (2019). An overview on joining of aluminium and magnesium alloys using friction stir welding (FSW) for automotive lightweight applications. Materials Research Express, 6(11), 112005.
21. Sharma, S.K.; Saxena, K.K. An outlook on the influence on mechanical properties of AZ31 reinforced with graphene nanoparticles using powder metallurgy technique for biomedical application. Mater. Today Proc. 2022, 56, 2278–2287.
22. Sharma, S.K.; Saxena, K.K.; Kumar, K.B.; Kumar, N. The effect of reinforcements on the mechanical properties of AZ31 composites prepared by powder metallurgy: An overview. Mater. Today Proc. 2022, 56, 2293–2299.
23. Alaneme, K. K., Kareem, S. A., Olajide, J. L., Sadiku, R. E., & Bodunrin, M. O. (2022). Computational biomechanical and biodegradation integrity assessment of Mg-based biomedical devices for cardiovascular and orthopedic applications: A Review. International Journal of Lightweight Materials and Manufacture.
24. Kulekci, M. K. (2008). Magnesium and its alloys applications in automotive industry. *The International Journal of Advanced Manufacturing Technology*, *39*(9), 851-865.
25. Sharma, S.K., Saxena, K.K., Malik, V, Mohammed, K.A., Prakash, C., Buddhi, D., Dixit, S. Significance of Alloying Elements on the Mechanical Characteristics of Mg-Based Materials for Biomedical Applications. Crystals 2022, 12, 1138.
26. Thompson, Mary Kathryn, Giovanni Moroni, Tom Vaneker, Georges Fadel, R. Ian Campbell, Ian Gibson, Alain Bernard et al. "Design for Additive Manufacturing: Trends, opportunities, considerations, and constraints." *CIRP annals* 65, no. 2 (2016): 737-760.
27. Zeng, Zhuoran, Mojtaba Salehi, Alexander Kopp, Shiwei Xu, Marco Esmaily, and Nick Birbilis. "Recent progress and perspectives in additive manufacturing of magnesium alloys." *Journal of Magnesium and Alloys* (2022).
28. Ning, Chengyun, Zhengnan Zhou, Guoxin Tan, Ye Zhu, and Chuanbin Mao. "Electroactive polymers for tissue regeneration: Developments and perspectives." *Progress in polymer science* 81 (2018): 144-162.
29. Ansari, Aftab Alam, Aleksandra Golebiowska, Madhusmita Dash, Prasoon Kumar, Prashant Kumar Jain, Syam Nukavarapu, Seeram Ramakrishna, and Himansu Sekhar Nanda. "Engineering biomaterials to 3D-print scaffolds for bone regeneration: practical and theoretical consideration." *Biomaterials Science* (2022).
30. Putra, N. E., M. J. Mirzaali, I. Apachitei, Jie Zhou, and A. A. Zadpoor. "Multi-material additive manufacturing technologies for Ti-, Mg-, and Fe-based biomaterials for bone substitution." *Acta biomaterialia* 109 (2020): 1-20.
31. Murty, B. S., and S. J. M. R. Ranganathan. "Novel materials synthesis by mechanical alloying/milling." *International materials reviews* 43, no. 3 (1998): 101-141.

32. Gu, Dong Dong, Wilhelm Meiners, Konrad Wissenbach, and Reinhart Poprawe. "Laser additive manufacturing of metallic components: materials, processes and mechanisms." *International materials reviews* 57, no. 3 (2012): 133-164.
33. Esmaily, Mohsen, Zhuoran Zeng, A. N. Mortazavi, Alessio Gullino, Sanjay Choudhary, Thomas Derra, Felix Benn et al. "A detailed microstructural and corrosion analysis of magnesium alloy WE43 manufactured by selective laser melting." *Additive Manufacturing* 35 (2020): 101321.
34. Santecchia, Eleonora, Stefano Spigarelli, and Marcello Cabibbo. "Material reuse in laser powder bed fusion: side effects of the laser—metal powder interaction." *Metals* 10, no. 3 (2020): 341.
35. Gradl, Paul R., Darren C. Tinker, John Ivester, Shawn W. Skinner, Thomas Teasley, and John L. Bili. "Geometric feature reproducibility for laser powder bed fusion (L-PBF) additive manufacturing with Inconel 718." *Additive Manufacturing* 47 (2021): 102305.
36. Gordon, Jerard V., Sneha P. Narra, Ross W. Cunningham, He Liu, Hangman Chen, Robert M. Suter, Jack L. Beuth, and Anthony D. Rollett. "Defect structure process maps for laser powder bed fusion additive manufacturing." *Additive Manufacturing* 36 (2020): 101552.\
37. Tekumalla, Sravya, Yogesh Nandigam, Nitish Bibhanshu, Shabadi Rajashekara, Chen Yang, Satyam Suwas, and Manoj Gupta. "A strong and deformable in-situ magnesium nanocomposite igniting above 1000 C." *Scientific reports* 8, no. 1 (2018): 1-10.
38. Wang, Hung-Yu, Yu-Lung Lo, Hong-Chuong Tran, M. Mohsin Raza, and Trong-Nhan Le. "Systematic approach for reducing micro-crack formation in Inconel 713LC components fabricated by laser powder bed fusion." *Rapid Prototyping Journal* (2021).
39. Deng, Qingchen, Yujuan Wu, Qianye Wu, Yanting Xue, Yu Zhang, Liming Peng, and Wenjiang Ding. "Microstructure evolution and mechanical properties of a high-strength Mg-10Gd-3Y–1Zn-0.4 Zr alloy fabricated by laser powder bed fusion." *Additive Manufacturing* 49 (2022): 102517.
40. Zhao, Chao, Zhi Wang, Daoxi Li, Meishen Xie, Lauri Kollo, Zongqiang Luo, Weiwen Zhang, and Konda Gokuldoss Prashanth. "Comparison of additively manufacturing samples fabricated from pre-alloyed and mechanically mixed powders." *Journal of Alloys and Compounds* 830 (2020): 154603.
41. Babu, A. P., S. K. Kairy, A. Huang, and N. Birbilis. "Laser powder bed fusion of high solute Al-Zn-Mg alloys: Processing, characterisation and properties." *Materials & Design* 196 (2020): 109183.
42. Niu, Xiaomiao, Hongyao Shen, Guanhua Xu, Linchu Zhang, Jianzhong Fu, and Xiaolei Deng. "Effect of aluminium content and processing parameters on the microstructure and mechanical properties of laser powder-bed fused magnesium-aluminium (0, 3, 6, 9wt%) powder mixture." *Rapid Prototyping Journal* 25, no. 4 (2019): 744-751.
43. Ron, Tomer, Avi Leon, Vladimir Popov, Evgeny Strokin, Dan Eliezer, Amnon Shirizly, and Eli Aghion. "Synthesis of Refractory High-Entropy Alloy WTaMoNbV by Powder Bed Fusion Process Using Mixed Elemental Alloying Powder." *Materials* 15, no. 12 (2022): 4043.
44. Niu, Xiaomiao, Hongyao Shen, Jianzhong Fu, Jinwen Yan, and Yu Wang. "Corrosion behaviour of laser powder bed fused bulk pure magnesium in hank's solution." *Corrosion Science* 157 (2019): 284-294.
45. Hu, Dong, Yong Wang, Dingfei Zhang, Liang Hao, Junjie Jiang, Zhonghua Li, and Yitao Chen. "Experimental investigation on selective laser melting of bulk net-shape pure magnesium." *Materials and Manufacturing Processes* 30, no. 11 (2015): 1298-1304.
46. Zhang, Baicheng, Hanlin Liao, and Christian Coddet. "Effects of processing parameters on properties of selective laser melting Mg–9% Al powder mixture." *Materials & Design* 34 (2012): 753-758.

47. Niu, Xiaomiao, Hongyao Shen, and Jianzhong Fu. "Microstructure and mechanical properties of selective laser melted Mg-9 wt% Al powder mixture." *Materials Letters* 221 (2018): 4-7.
48. Liu, Shuai, WenSheng Yang, Xiao Shi, Bin Li, Shengchao Duan, Hanjie Guo, and Jing Guo. "Influence of laser process parameters on the densification, microstructure, and mechanical properties of a selective laser melted AZ61 magnesium alloy." *Journal of Alloys and Compounds* 808 (2019): 151160.
49. He, Chongxian, Shizhen Bin, Ping Wu, Chengde Gao, Pei Feng, Youwen Yang, Long Liu et al. "Microstructure evolution and biodegradation behavior of laser rapid solidified Mg–Al–Zn alloy." *Metals* 7, no. 3 (2017): 105.
50. Wei, Kaiwen, Ming Gao, Zemin Wang, and Xiaoyan Zeng. "Effect of energy input on formability, microstructure and mechanical properties of selective laser melted AZ91D magnesium alloy." *Materials Science and Engineering: A* 611 (2014): 212-222.
51. Zhu, Z., M. Zhang, and C. Chen. "Effect of selective laser melting on microstructure and properties of AZ91D alloy." *Materialwissenschaft und Werkstofftechnik* 50, no. 12 (2019): 1484-1494.
52. Jauer, Lucas, Wilhelm Meiners, Simon Vervoort, Christoph Gayer, Naemi A. Zumdick, and Daniela Zander. "Selective laser melting of magnesium alloys." In *European Congress and Exhibition on Powder Metallurgy. European PM Conference Proceedings*, pp. 1-6. The European Powder Metallurgy Association, 2016.
53. Niu, Xiaomiao, Hongyao Shen, Jianzhong Fu, and Jiawei Feng. "Effective control of microstructure evolution in AZ91D magnesium alloy by SiC nanoparticles in laser powder-bed fusion." *Materials & Design* 206 (2021): 109787.
54. Zumdick, Naemi A., Lucas Jauer, Lisa C. Kersting, Tatiana N. Kutz, Johannes H. Schleifenbaum, and Daniela Zander. "Additive manufactured WE43 magnesium: A comparative study of the microstructure and mechanical properties with those of powder extruded and as-cast WE43." *Materials Characterization* 147 (2019): 384-397.
55. Hyer, Holden, Le Zhou, George Benson, Brandon McWilliams, Kyu Cho, and Yongho Sohn. "Additive manufacturing of dense WE43 Mg alloy by laser powder bed fusion." *Additive Manufacturing* 33 (2020): 101123.
56. Bär, Florian, Leopold Berger, Lucas Jauer, Güven Kurtuldu, Robin Schäublin, Johannes H. Schleifenbaum, and Jörg F. Löffler. "Laser additive manufacturing of biodegradable magnesium alloy WE43: a detailed microstructure analysis." *Acta biomaterialia* 98 (2019): 36-49.
57. Gangireddy, Sindhura, Bharat Gwalani, Kaimiao Liu, Eric J. Faierson, and Rajiv S. Mishra. "Microstructure and mechanical behavior of an additive manufactured (AM) WE43-Mg alloy." *Additive Manufacturing* 26 (2019): 53-64.
58. Deng, Qingchen, Yujuan Wu, Ning Su, Zhiyu Chang, Juan Chen, Liming Peng, and Wenjiang Ding. "Influence of friction stir processing and aging heat treatment on microstructure and mechanical properties of selective laser melted Mg-Gd-Zr alloy." *Additive Manufacturing* 44 (2021): 102036.
59. Deng, Qingchen, Yujuan Wu, Yuanhang Luo, Ning Su, Xiaoyu Xue, Zhiyu Chang, Qianye Wu, Yanting Xue, and Liming Peng. "Fabrication of high-strength Mg-Gd-Zn-Zr alloy via selective laser melting." *Materials Characterization* 165 (2020): 110377.
60. Fu, Peng-huai, Nan-qing Wang, Hai-guang Liao, Wen-yu Xu, Li-ming Peng, C. H. E. N. Juan, Guo-qi Hu, and Wen-jiang Ding. "Microstructure and mechanical properties of high strength Mg− 15Gd− 1Zn− 0.4 Zr alloy additive-manufactured by selective laser melting process." *Transactions of Nonferrous Metals Society of China* 31, no. 7 (2021): 1969-1978.
61. Wei, Kaiwen, Xiaoyan Zeng, Zemin Wang, Jinfeng Deng, Mengna Liu, Gao Huang, and Xiaochi Yuan. "Selective laser melting of Mg-Zn binary alloys: Effects of Zn content on densification behavior, microstructure, and mechanical property." *Materials Science and Engineering: A* 756 (2019): 226-236.

62. Wei, Kaiwen, Zemin Wang, and Xiaoyan Zeng. "Influence of element vaporization on formability, composition, microstructure, and mechanical performance of the selective laser melted Mg–Zn–Zr components." *Materials Letters* 156 (2015): 187-190.
63. Yang, Kyung-Tae, Min-Kyeom Kim, Dongwon Kim, and Jonghwan Suhr. "Investigation of laser powder bed fusion manufacturing and post-processing for surface quality of as-built 17-4PH stainless steel." *Surface and Coatings Technology* 422 (2021): 127492.
64. Megahed, Mustafa, Hans-Wilfried Mindt, Jöerg Willems, Paul Dionne, Lars Jacquemetton, James Craig, Piyush Ranade, and Alonso Peralta. "LPBF right the first time—The right mix between modeling and experiments." *Integrating Materials and Manufacturing Innovation* 8, no. 2 (2019): 194-216.
65. Prasad, Kartik, Mitsuki Obana, Yuki Ishii, Atsushi Ito, and Shiro Torizuka. "The effect of laser scanning strategies on the microstructure, texture and crystallography of grains exhibiting hot cracks in additively manufactured Hastelloy X." *Mechanics of Materials* 157 (2021): 103816.
66. Nabawy, A. M., A. M. Samuel, F. H. Samuel, and H. W. Doty. "Influence of additions of Zr, Ti–B, Sr, and Si as well as of mold temperature on the hot-tearing susceptibility of an experimental Al–2% Cu–1% Si alloy." *Journal of materials science* 47, no. 9 (2012): 4146-4158.
67. Qin, He, Guang-yu Yang, Xun-wei Zheng, Shi-feng Luo, Tong Bai, and Wan-qi Jie. "Effect of Gd content on hot-tearing susceptibility of Mg-6Zn-xGd casting alloys." *China Foundry* 19, no. 2 (2022): 131-139.
68. Park, Sung Soo, W-J. Park, C. H. Kim, B. S. You, and Nack J. Kim. "The twin-roll casting of magnesium alloys." *JOM* 61, no. 8 (2009): 14-18.
69. Maeng, D. Y., T. S. Kim, J. H. Lee, S. J. Hong, S. K. Seo, and B. S. Chun. "Microstructure and strength of rapidly solidified and extruded Mg-Zn alloys." *Scripta materialia* 43, no. 5 (2000): 385-389.
70. Yang, Yan, Xiaoming Xiong, Jing Chen, Xiaodong Peng, Daolun Chen, and Fusheng Pan. "Research advances in magnesium and magnesium alloys worldwide in 2020." *Journal of Magnesium and Alloys* 9, no. 3 (2021): 705-747.
71. Patel, Bhumi K., Falak P. Patel, and Vishvesh J. Badheka. "Review on Friction-Based Additive Manufacturing Processes: Types, Defects, and Applications." In *Recent Advances in Manufacturing Processes and Systems*, pp. 885-903. Springer, Singapore, 2022.
72. Karunakaran, Rakeshkumar, Sam Ortgies, Ryan Green, William Barelman, Ian Kobler, and Michael Sealy. "Accelerated Corrosion Behavior of Additive Manufactured WE43 Magnesium Alloy." In *2021 International Solid Freeform Fabrication Symposium*. University of Texas at Austin, 2021.
73. Cao, Xin-jin, M. Jahazi, J. P. Immarigeon, and W. Wallace. "A review of laser welding techniques for magnesium alloys." *Journal of Materials Processing Technology* 171, no. 2 (2006): 188-204.
74. Zhang, Z., Tan, Z.J., Li, J.Y., Zu, Y.F., Liu, W.W. and Sha, J.J., 2019. Experimental and numerical studies of re-stirring and re-heating effects on mechanical properties in friction stir additive manufacturing. *The International Journal of Advanced Manufacturing Technology*, *104*(1), pp.767-784.
75. Cedeño-Viveros, Luis D., Luis H. Olivas-Alanis, Omar Lopez-Botello, Ciro A. Rodriguez, Elisa Vazquez-Lepe, and Erika García-López. "A novel method for the fabrication of tubular WE43 magnesium scaffold based on laser micro-spot welding." *Engineering Science and Technology, an International Journal* 34 (2022): 101096.
76. Sekar, Prithivirajan, S. Narendranath, and Vijay Desai. "Recent progress in in vivo studies and clinical applications of magnesium based biodegradable implants–a review." *Journal of Magnesium and Alloys* 9, no. 4 (2021): 1147-1163.

77. Nagarajan, Balasubramanian, Zhiheng Hu, Xu Song, Wei Zhai, and Jun Wei. "Development of micro selective laser melting: The state of the art and future perspectives." *Engineering* 5, no. 4 (2019): 702-720.
78. Soderlind, Julie Christine. "Alternative Processing Methods for Mg Alloy WE43." PhD diss., University of California, Davis, 2020.
79. Sun, H. Q., Y-N. Shi, M-X. Zhang, and K. Lu. "Plastic strain-induced grain refinement in the nanometer scale in a Mg alloy." *Acta Materialia* 55, no. 3 (2007): 975-982.
80. Estrin, Yuri, and Alexei Vinogradov. "Extreme grain refinement by severe plastic deformation: A wealth of challenging science." *Acta materialia* 61, no. 3 (2013): 782-817.
81. Stopyra, Wojciech, Konrad Gruber, Irina Smolina, Tomasz Kurzynowski, and Bogumiła Kuźnicka. "Laser powder bed fusion of AA7075 alloy: Influence of process parameters on porosity and hot cracking." *Additive Manufacturing* 35 (2020): 101270.
82. Sanchez, Salomé, Peter Smith, Zhengkai Xu, Gabriele Gaspard, Christopher J. Hyde, Wessel W. Wits, Ian A. Ashcroft, Hao Chen, and Adam T. Clare. "Powder Bed Fusion of nickel-based superalloys: A review." *International Journal of Machine Tools and Manufacture* 165 (2021): 103729.
83. Talignani, Alberico, Raiyan Seede, Austin Whitt, Shiqi Zheng, Jianchao Ye, Ibrahim Karaman, Michael M. Kirka, Yutai Kato, and Y. Morris Wang. "A review on additive manufacturing of refractory tungsten and tungsten alloys." *Additive Manufacturing* (2022): 103009.
84. Field, Amanda Catherine. "Laser Powderbed Fusion (LPBF) of tungsten and tungsten alloys for nuclear fusion applications." PhD diss., University of Birmingham, 2020.
85. Irrinki, Harish. "Material-process-property relationships of 17-4 stainless steel fabricated by laser-powder bed fusion followed by hot isostatic pressing." (2018).
86. Dunbar, A. J., E. R. Denlinger, J. Heigel, P. Michaleris, P. Guerrier, R. Martukanitz, and T. W. Simpson. "Development of experimental method for in situ distortion and temperature measurements during the laser powder bed fusion additive manufacturing process." *Additive Manufacturing* 12 (2016): 25-30.
87. Levkulich, N. C., S. L. Semiatin, J. E. Gockel, J. R. Middendorf, A. T. DeWald, and N. W. Klingbeil. "The effect of process parameters on residual stress evolution and distortion in the laser powder bed fusion of Ti-6Al-4V." *Additive Manufacturing* 28 (2019): 475-484.
88. Nakata, T., C. Xu, H. Ohashi, Y. Yoshida, K. Yoshida, and S. Kamado. "New Mg–Al based alloy sheet with good room-temperature stretch formability and tensile properties." *Scripta Materialia* 180 (2020): 16-22.
89. ZHANG, Aimin, H. A. O. Hai, L. I. U. Xiaoteng, and Xingguo ZHANG. "Effects of precipitates on grain size and mechanical properties of AZ31-x% Nd magnesium alloy." *Journal of Rare Earths* 32, no. 5 (2014): 451-457.
90. Ali, Yahia, Dong Qiu, Bin Jiang, Fusheng Pan, and Ming-Xing Zhang. "Current research progress in grain refinement of cast magnesium alloys: A review article." *Journal of Alloys and Compounds* 619 (2015): 639-651.
91. Jana, Saumyadeep, Matt Olszta, Danny Edwards, Mark Engelhard, Avik Samanta, Hongtao Ding, Pratik Murkute, O. Burkan Isgor, and Aashish Rohatgi. "Microstructural basis for improved corrosion resistance of laser surface processed AZ31 Mg alloy." *Corrosion Science* 191 (2021): 109707.
92. Luo, Alan A., Anil K. Sachdev, and Diran Apelian. "Alloy development and process innovations for light metals casting." *Journal of Materials Processing Technology* (2022): 117606.

93. Deng, Qingchen, Xingchen Wang, Qiao Lan, Zhiyu Chang, Zehua Liu, Ning Su, Yujuan Wu, Dazhi Liu, Liming Peng, and Wenjiang Ding. "Limitations of linear energy density for laser powder bed fusion of Mg-15Gd-1Zn-0.4 Zr alloy." *Materials Characterization* 190 (2022): 112071.
94. Motallebi, Reza, Zeinab Savaedi, and Hamed Mirzadeh. "Post-processing heat treatment of lightweight magnesium alloys fabricated by additive manufacturing: A review." *Journal of Materials Research and Technology* (2022).
95. Kong, Decheng, Chaofang Dong, Shaolou Wei, Xiaoqing Ni, Liang Zhang, Ruixue Li, Li Wang, Cheng Man, and Xiaogang Li. "About metastable cellular structure in additively manufactured austenitic stainless steels." *Additive Manufacturing* 38 (2021): 101804.
96. Luo, X., D. D. Li, C. Yang, A. Gebert, H. Z. Lu, T. Song, H. W. Ma, L. M. Kang, Y. Long, and Y. Y. Li. "Circumventing the strength–ductility trade-off of β-type titanium alloys by defect engineering during laser powder bed fusion." *Additive Manufacturing* 51 (2022): 102640.
97. Ma, X. L., Suhas Eswarappa Prameela, Peng Yi, Matthew Fernandez, Nicholas M. Krywopusk, Laszlo J. Kecskes, Tomoko Sano, Michael L. Falk, and Timothy P. Weihs. "Dynamic precipitation and recrystallization in Mg-9wt.% Al during equal-channel angular extrusion: A comparative study to conventional aging." *Acta Materialia* 172 (2019): 185-199.
98. Maghsoudi, M. H., A. Zarei-Hanzaki, H. R. Abedi, and A. Shamsolhodaei. "The evolution of γ-Mg17Al12 intermetallic compound during accumulative back extrusion and subsequent ageing treatment." *Philosophical Magazine* 95, no. 31 (2015): 3497-3523.
99. Cifuentes, Sandra Carolina, and Sala Grados Auditorio Padre Soler. "Processing and characterization of novel biodegradable and bioresorbable PLA/Mg composites for osteosynthesis." PhD diss., 2015.
100. Cifuentes Cuéllar, Sandra Carolina. "Processing and characterization of novel biodegradable and bioresorbable PLA/Mg composites for osteosynthesis." (2015).
101. Zhang, Xiang, Fei Wang, Xueliang Yan, Xing-Zhong Li, Khalid Hattar, and Bai Cui. "Nanostructured Oxide-Dispersion-Strengthened CoCrFeMnNi High-Entropy Alloys with High Thermal Stability." *Advanced Engineering Materials* 23, no. 9 (2021): 2100291.
102. Murty, Budaraju S., P. Shankar, Baldev Raj, B. B. Rath, and James Murday. *Textbook of nanoscience and nanotechnology*. Springer Science & Business Media, 2013.
103. Sharma, S.K.; Saxena, K.K. Effects on microstructure and mechanical properties of AZ31 reinforced with CNT by powder metallurgy: An overview. Mater. Today Proc. 2022, 56, 2038–2042.
104. Khojastehnezhad, Vahid Mohammadzadeh. "Microstructures and Mechanical Properties of Al 6061/Al2O3-TiB2 Hybrid Nano-Composite layer Produced via Friction Stir Processing Using Optimized Process Parameters." (2019).
105. Sahu, Manas Ranjan, TS Sampath Kumar, and Uday Chakkingal. "A review on recent advancements in biodegradable Mg-Ca alloys." *Journal of Magnesium and Alloys* (2022).
106. Easton, Mark, and David StJohn. "An analysis of the relationship between grain size, solute content, and the potency and number density of nucleant particles." *Metallurgical and materials transactions A* 36, no. 7 (2005): 1911-1920.
107. Hänzi, Anja C., Alla S. Sologubenko, and Peter J. Uggowitzer. "Design strategy for microalloyed ultra-ductile magnesium alloys for medical applications." In *Materials Science Forum*, vol. 618, pp. 75-82. Trans Tech Publications Ltd, 2009.
108. Easton, Mark Alan, and David H. StJohn. "A model of grain refinement incorporating alloy constitution and potency of heterogeneous nucleant particles." *Acta Materialia* 49, no. 10 (2001): 1867-1878.
109. Robson, J. D., and P. B. Prangnell. "Dispersoid precipitation and process modelling in zirconium containing commercial aluminium alloys." *Acta Materialia* 49, no. 4 (2001): 599-613.

110. Robson, J. D., and P. B. Prangnell. "Dispersoid precipitation and process modelling in zirconium containing commercial aluminium alloys." *Acta Materialia* 49, no. 4 (2001): 599-613.
111. McGhee, Paul. "Effect of Microstructure on the Mechanical Properties of Extruded Magnesium and a Magnesium Alloy." PhD diss., North Carolina Agricultural and Technical State University, 2017.
112. Sharma, S.K.; Saxena, K.K. Effects on microstructure and mechanical properties of AZ31 reinforced with CNT by powder metallurgy: An overview. Mater. Today Proc. 2022, 56, 2038–2042.
113. Liou, Tzong-Horng. "Preparation and characterization of nano-structured silica from rice husk." *Materials Science and Engineering: A* 364, no. 1-2 (2004): 313-323.
114. Burton, Allen W., Kenneth Ong, Thomas Rea, and Ignatius Y. Chan. "On the estimation of average crystallite size of zeolites from the Scherrer equation: A critical evaluation of its application to zeolites with one-dimensional pore systems." *Microporous and Mesoporous Materials* 117, no. 1-2 (2009): 75-90.
115. Fan, Lili, Ming Xue, Zixi Kang, Huan Li, and Shilun Qiu. "Electrospinning technology applied in zeolitic imidazolate framework membrane synthesis." *Journal of Materials Chemistry* 22, no. 48 (2012): 25272-25276.
116. Azwa, Z. N., B. F. Yousif, A. C. Manalo, and W. Karunasena. "A review on the degradability of polymeric composites based on natural fibres." *Materials & Design* 47 (2013): 424-442.
117. Rometsch, Paul A., Yuman Zhu, Xinhua Wu, and Aijun Huang. "Review of High-Strength Aluminium Alloys for Additive Manufacturing by Laser Powder Bed Fusion." *Materials & Design* (2022): 110779.
118. Clemens, Helmut, and Svea Mayer. "Design, processing, microstructure, properties, and applications of advanced intermetallic TiAl alloys." *Advanced engineering materials* 15, no. 4 (2013): 191-215.
119. Mertens, Anne I., Jocelyn Delahaye, and Jacqueline Lecomte-Beckers. "Fusion-based additive manufacturing for processing aluminum alloys: State-of-the-art and challenges." *Advanced Engineering Materials* 19, no. 8 (2017): 1700003.
120. Singla, Anil Kumar, Mainak Banerjee, Aman Sharma, Jagtar Singh, Anuj Bansal, Munish Kumar Gupta, Navneet Khanna, A. S. Shahi, and Deepak Kumar Goyal. "Selective laser melting of Ti6Al4V alloy: Process parameters, defects and post-treatments." *Journal of Manufacturing Processes* 64 (2021): 161-187.
121. Buttard, Maxence, Béchir Chehab, Ravi Shahani, Florence Robaut, Gilles Renou, Catherine Tassin, Edgar Rauch et al. "Multi-scale microstuctural investigation of a new Al-Mn-Ni-Cu-Zr aluminium alloy processed by laser powder bed fusion." *Materialia* 18 (2021): 101160.
122. Marchese, Giulio, Massimo Lorusso, Simone Parizia, Emilio Bassini, Ji-Won Lee, Flaviana Calignano, Diego Manfredi et al. "Influence of heat treatments on microstructure evolution and mechanical properties of Inconel 625 processed by laser powder bed fusion." *Materials Science and Engineering: A* 729 (2018): 64-75.
123. Terner, Mathieu, Jiwon Lee, Giulio Marchese, Sara Biamino, and Hyun-Uk Hong. "Electron backscattered diffraction to estimate residual stress levels of a superalloy produced by laser powder bed fusion and subsequent heat treatments." *Materials* 13, no. 20 (2020): 4643.
124. Dzogbewu, Thywill Cephas. "Additive manufacturing of TiAl-based alloys." *Manufacturing Review* 7 (2020): 35.
125. Cao, Sheng, Yichao Zou, Chao Voon Samuel Lim, and Xinhua Wu. "Review of laser powder bed fusion (LPBF) fabricated Ti-6Al-4V: process, post-process treatment, microstructure, and property." *Light: Advanced Manufacturing* 2, no. 3 (2021): 313-332.
126. Putra, N. E., K. G. N. Borg, P. J. Diaz-Payno, M. A. Leeflang, M. Klimopoulou, P. Taheri, J. M. C. Mol et al. "Additive manufacturing of bioactive and biodegradable porous iron-akermanite composites for bone regeneration." *Acta Biomaterialia* (2022).

127. Zhang, Baicheng, Hanlin Liao, and Christian Coddet. "Effects of processing parameters on properties of selective laser melting Mg–9% Al powder mixture." *Materials & Design* 34 (2012): 753-758.
128. Han, Hyung-Seop, Sergio Loffredo, Indong Jun, James Edwards, Yu-Chan Kim, Hyun-Kwang Seok, Frank Witte, Diego Mantovani, and Sion Glyn-Jones. "Current status and outlook on the clinical translation of biodegradable metals." *Materials Today* 23 (2019): 57-71.
129. Zamani, Yasamin, Hadi Ghazanfari, Gisou Erabi, Amirhossein Moghanian, Belma Fakić, Seyed Mohammad Hosseini, and Babar Pasha Mahammod. "A review of additive manufacturing of Mg-based alloys and composite implants." *Journal of Composites and Compounds* 3, no. 6 (2021): 71-83.
130. Okoro, Victor Udochukwu. "Irradiation assisted corrosion of cast A360. 1 and additively manufactured AlSi10Mg aluminum alloys in seawater environments." PhD diss., University of New Brunswick., 2021.
131. Li, Muzi, Felix Benn, Thomas Derra, Nadja Kröger, Max Zinser, Ralf Smeets, Jon M. Molina-Aldareguia, Alexander Kopp, and Javier LLorca. "Microstructure, mechanical properties, corrosion resistance and cytocompatibility of WE43 Mg alloy scaffolds fabricated by laser powder bed fusion for biomedical applications." *Materials Science and Engineering: C* 119 (2021): 111623.
132. Song, Guan Ling, and Andrej Atrens. "Corrosion mechanisms of magnesium alloys." *Advanced engineering materials* 1, no. 1 (1999): 11-33.
133. Sezer, Nurettin, Zafer Evis, and Muammer Koc. "Additive manufacturing of biodegradable magnesium implants and scaffolds: Review of the recent advances and research trends." *Journal of Magnesium and Alloys* 9, no. 2 (2021): 392-415.
134. Das, Priyabrata, TS Sampath Kumar, Kisor K. Sahu, and Srikant Gollapudi. "Corrosion, stress corrosion cracking and corrosion fatigue behavior of magnesium alloy bioimplants." *Corrosion Reviews* (2022).
135. Liang, Jingwei, Zhenglong Lei, Yanbin Chen, Weijie Fu, Shibo Wu, Xi Chen, and Yuchen Yang. "Microstructure evolution of laser powder bed fusion ZK60 Mg alloy after different heat treatment." *Journal of Alloys and Compounds* 898 (2022): 163046.
136. Zeng, Rongchang, Wolfgang Dietzel, Frank Witte, Norbert Hort, and Carsten Blawert. "Progress and challenge for magnesium alloys as biomaterials." *Advanced engineering materials* 10, no. 8 (2008): B3-B14.
137. Zhang, Y. Z., J. Venugopal, Z-M. Huang, C. T. Lim, and S. Ramakrishna. "Characterization of the surface biocompatibility of the electrospun PCL-collagen nanofibers using fibroblasts." *Biomacromolecules* 6, no. 5 (2005): 2583-2589.
138. Gutierrez, Elena, Patricio A. Burdiles, Franck Quero, Patricia Palma, Felipe Olate-Moya, and Humberto Palza. "3D printing of antimicrobial alginate/bacterial-cellulose composite hydrogels by incorporating copper nanostructures." *ACS Biomaterials Science & Engineering* 5, no. 11 (2019): 6290-6299.
139. Ferrández-Montero, Ana, Marcela Lieblich, José Luis González-Carrasco, Rosario Benavente, and Bruno Ferrari. "Tailoring biodegradable and bioactive polymer/Mg composites for additive manufacturing." (2019).
140. Md Yusop, Abdul Hakim, Ahmed Al Sakkaf, and Hadi Nur. "Modifications on porous absorbable Fe-based scaffolds for bone applications: A review from corrosion and biocompatibility viewpoints." *Journal of Biomedical Materials Research Part B: Applied Biomaterials* 110, no. 1 (2022): 18-44.
141. Nair, Manitha B., H. K. Varma, P. V. Mohanan, and Annie John. "Tissue-engineered triphasic ceramic coated hydroxyapatite induced bone formation and vascularization at an extraskeletal site in a rat model." *Bulletin of Materials Science* 34, no. 7 (2011): 1721-1731.
142. Bartolomeu, F., Miguel Sampaio, O. Carvalho, E. Pinto, N. Alves, J. R. Gomes, Filipe Samuel Silva, and G. Miranda. "Tribological behavior of Ti6Al4V cellular structures produced by Selective Laser Melting." *Journal of the mechanical behavior of biomedical materials* 69 (2017): 128-134.

143. Yeo, Seon Ju, Min Jun Oh, and Pil J. Yoo. "Structurally controlled cellular architectures for high-performance ultra-lightweight materials." *Advanced Materials* 31, no. 34 (2019): 1803670.
144. Zhang, Jinliang, Bo Song, Qingsong Wei, Dave Bourell, and Yusheng Shi. "A review of selective laser melting of aluminum alloys: Processing, microstructure, property and developing trends." *Journal of Materials Science & Technology* 35, no. 2 (2019): 270-284.
145. Aboulkhair, Nesma T., Marco Simonelli, Luke Parry, Ian Ashcroft, Christopher Tuck, and Richard Hague. "3D printing of Aluminium alloys: Additive Manufacturing of Aluminium alloys using selective laser melting." *Progress in materials science* 106 (2019): 100578.
146. Huang, Junlin, Derek Lister, Shunsuke Uchida, and Lihui Liu. "The corrosion of aluminium alloy and release of intermetallic particles in nuclear reactor emergency core coolant: Implications for clogging of sump strainers." *Nuclear Engineering and Technology* 51, no. 5 (2019): 1345-1354.
147. Rometsch, Paul, Qingbo Jia, Kun V. Yang, and Xinhua Wu. "Aluminum alloys for selective laser melting–towards improved performance." In *Additive Manufacturing for the Aerospace Industry*, pp. 301-325. Elsevier, 2019.
148. Kalaiselvan, K., Natarajan Murugan, and Siva Parameswaran. "Production and characterization of AA6061–B4C stir cast composite." *Materials & Design* 32, no. 7 (2011): 4004-4009.
149. Han, Yanfeng, Xiangfa Liu, and Xiufang Bian. "In situ TiB2 particulate reinforced near eutectic Al–Si alloy composites." *Composites Part A: Applied Science and Manufacturing* 33, no. 3 (2002): 439-444.
150. Mohamed, A. M. A., and F. H. Samuel. "A review on the heat treatment of Al-Si-Cu/Mg casting alloys." In *Heat Treatment-Conventional and Novel Applications*, vol. 1, pp. 55-72. Rijeka, Croatia: InTech, 2012.
151. Shaha, S. K., F. Czerwinski, W. Kasprzak, J. Friedman, and D. L. Chen. "Microstructure and mechanical properties of Al–Si cast alloy with additions of Zr–V–Ti." *Materials & Design* 83 (2015): 801-812.
152. Sadrekarimi, Abouzar. "Development of a light weight reactive powder concrete." *Journal of Advanced Concrete Technology* 2, no. 3 (2004): 409-417.
153. Aboulkhair, Nesma T., Nicola M. Everitt, Ian Maskery, Ian Ashcroft, and Chris Tuck. "Selective laser melting of aluminum alloys." *MRS Bulletin* 42, no. 4 (2017): 311-319.
154. Rometsch, Paul, Qingbo Jia, Kun V. Yang, and Xinhua Wu. "1Department of Materials Science and Engineering, Monash University, Clayton, VIC, Australia, 2Monash Centre for Additive Manufacturing (MCAM), Monash University, Notting Hill, VIC, Australia, 3Rio Tinto Arvida Research and Development Centre, Jonquiere, QC, Canada, 4CSIRO Manufacturing, Clayton, VIC, Australia." *Additive Manufacturing for the Aerospace Industry* (2019): 301.
155. Harrison, Neil J., Iain Todd, and Kamran Mumtaz. "Reduction of micro-cracking in nickel superalloys processed by Selective Laser Melting: A fundamental alloy design approach." *Acta Materialia* 94 (2015): 59-68.
156. Li, C., R. White, X. Y. Fang, M. Weaver, and Y. B. Guo. "Microstructure evolution characteristics of Inconel 625 alloy from selective laser melting to heat treatment." *Materials Science and Engineering: A* 705 (2017): 20-31.
157. Thijs, Lore, Maria Luz Montero Sistiaga, Ruben Wauthle, Qingge Xie, Jean-Pierre Kruth, and Jan Van Humbeeck. "Strong morphological and crystallographic texture and resulting yield strength anisotropy in selective laser melted tantalum." *Acta Materialia* 61, no. 12 (2013): 4657-4668.
158. Deng, Dunyong, Ru Lin Peng, Håkan Brodin, and Johan Moverare. "Microstructure and mechanical properties of Inconel 718 produced by selective laser melting: Sample orientation dependence and effects of post heat treatments." *Materials Science and Engineering: A* 713 (2018): 294-306.

159. Aboulkhair, Nesma T., Ian Maskery, Chris Tuck, Ian Ashcroft, and Nicola M. Everitt. "On the formation of AlSi10Mg single tracks and layers in selective laser melting: Microstructure and nano-mechanical properties." *Journal of Materials Processing Technology* 230 (2016): 88-98.
160. Lu, Xin, Xiaoyi Yang, Xin Zhao, Hongbin Yang, and Mengnie Victor Li. "Additively manufactured AlSi10Mg ultrathin walls: Microstructure and nano-mechanical properties under different energy densities and interlayer cooling times." *Materials Science and Engineering: A* 835 (2022): 142652.
161. Aboulkhair, Nesma T., Ian Maskery, Chris Tuck, Ian Ashcroft, and Nicola M. Everitt. "The microstructure and mechanical properties of selectively laser melted AlSi10Mg: The effect of a conventional T6-like heat treatment." *Materials Science and Engineering: A* 667 (2016): 139-146.
162. Aboulkhair, Nesma T., Marco Simonelli, Ehab Salama, Graham A. Rance, Nigel C. Neate, Christopher J. Tuck, Amal MK Esawi, and Richard JM Hague. "Evolution of carbon nanotubes and their metallurgical reactions in Al-based composites in response to laser irradiation during selective laser melting." *Materials Science and Engineering: A* 765 (2019): 138307.
163. Wei, Pei, Zhengying Wei, Zhen Chen, Jun Du, Yuyang He, Junfeng Li, and Yatong Zhou. "The AlSi10Mg samples produced by selective laser melting: single track, densification, microstructure and mechanical behavior." *Applied surface science* 408 (2017): 38-50.
164. Wang, Y. L., L. Zhao, Di Wan, Shuai Guan, and K. C. Chan. "Additive manufacturing of TiB2-containing CoCrFeMnNi high-entropy alloy matrix composites with high density and enhanced mechanical properties." *Materials Science and Engineering: A* 825 (2021): 141871.
165. Shakil, S. I., A. Hadadzadeh, B. Shalchi Amirkhiz, H. Pirgazi, M. Mohammadi, and M. Haghshenas. "Additive manufactured versus cast AlSi10Mg alloy: Microstructure and micromechanics." *Results in Materials* 10 (2021): 100178.
166. Alghamdi, F., and M. Haghshenas. "Microstructural and small-scale characterization of additive manufactured AlSi10Mg alloy." *SN Applied Sciences* 1, no. 3 (2019): 1-10.
167. Kim, Tae Hwan, Gyeong Yun Baek, Jong Bae Jeon, Ki Yong Lee, Do-sik Shim, and Wookjin Lee. "Effect of laser rescanning on microstructure and mechanical properties of direct energy deposited AISI 316L stainless steel." *Surface and Coatings Technology* 405 (2021): 126540.
168. Mahmood, Muhammad Arif, Diana Chioibasu, Asif Ur Rehman, Sabin Mihai, and Andrei C. Popescu. "Post-Processing Techniques to Enhance the Quality of Metallic Parts Produced by Additive Manufacturing." *Metals* 12, no. 1 (2022): 77.
169. Zhang, Duyao, Shoujin Sun, Dong Qiu, Mark A. Gibson, Matthew S. Dargusch, Milan Brandt, Ma Qian, and Mark Easton. "Metal alloys for fusion-based additive manufacturing." *Advanced Engineering Materials* 20, no. 5 (2018): 1700952.
170. Chung, Ding-Wen. "Effect of Lattice Misfit on Microstructural Evolution and Mechanical Properties in Gamma-Prime Strengthened Cobalt-Based Superalloys." PhD diss., Northwestern University, 2020.
171. Maamoun, Ahmed H., Mohamed Elbestawi, Goulnara K. Dosbaeva, and Stephen C. Veldhuis. "Thermal post-processing of AlSi10Mg parts produced by Selective Laser Melting using recycled powder." *Additive Manufacturing* 21 (2018): 234-247.
172. Cui, X., S. Zhang, C. H. Zhang, J. Chen, J. B. Zhang, and S. Y. Dong. "Additive manufacturing of 24CrNiMo low alloy steel by selective laser melting: influence of volumetric energy density on densification, microstructure and hardness." *Materials Science and Engineering: A* 809 (2021): 140957.
173. Alghamdi, F., X. Song, A. Hadadzadeh, B. Shalchi-Amirkhiz, M. Mohammadi, and M. Haghshenas. "Post heat treatment of additive manufactured AlSi10Mg: On silicon morphology, texture and small-scale properties." *Materials Science and Engineering: A* 783 (2020): 139296.

174. Riddle, Y. W., and T. H. Sanders. "A study of coarsening, recrystallization, and morphology of microstructure in Al-Sc-(Zr)-(Mg) alloys." *Metallurgical and Materials Transactions A* 35, no. 1 (2004): 341-350.
175. Shi, Yunjia, Qinglin Pan, Mengjia Li, Xing Huang, and Bo Li. "Effect of Sc and Zr additions on corrosion behaviour of Al–Zn–Mg–Cu alloys." *Journal of Alloys and Compounds* 612 (2014): 42-50.
176. Norman, A. F., P. B. Prangnell, and R. S. McEwen. "The solidification behaviour of dilute aluminium–scandium alloys." *Acta materialia* 46, no. 16 (1998): 5715-5732.
177. Wang, Lianfeng, Xiaohui Jiang, Miaoxian Guo, Xiaogang Zhu, and Biao Yan. "Characterisation of structural properties for AlSi10Mg alloys fabricated by selective laser melting." *Materials Science and Technology* 33, no. 18 (2017): 2274-2282.
178. El-Batahgy, Abdel-Monem, Olga Klimova-Korsmik, Aleksandr Akhmetov, and Gleb Turichin. "High-Power Fiber Laser Welding of High-Strength AA7075-T6 Aluminum Alloy Welds for Mechanical Properties Research." *Materials* 14, no. 24 (2021): 7498.
179. Martin, John H., Brennan D. Yahata, Jacob M. Hundley, Justin A. Mayer, Tobias A. Schaedler, and Tresa M. Pollock. "3D printing of high-strength aluminium alloys." *Nature* 549, no. 7672 (2017): 365-369.
180. Tiryakioğlu, Murat, and J. T. Staley. "Physical metallurgy and the effect of alloying additions in aluminum alloys." *Handbook of aluminum* 1 (2003): 81-210.
181. Li, Qiuge, Guichuan Li, Xin Lin, Daiman Zhu, Jinhang Jiang, Shuoqing Shi, Fenggang Liu, Weidong Huang, and Kim Vanmeensel. "Development of a high strength Zr/Sc/Hf-modified Al-Mn-Mg alloy using Laser Powder Bed Fusion: Design of a heterogeneous microstructure incorporating synergistic multiple strengthening mechanisms." *Additive Manufacturing* 57 (2022): 102967.
182. Del Castillo, Linda Yvonne. *The influence of spray deposition processing on the microstructure and mechanical behavior of aluminum-copper-magnesium-silver alloys*. University of California, Irvine, 2000.
183. Asgari, Hamed, Carter Baxter, Keyvan Hosseinkhani, and Mohsen Mohammadi. "On microstructure and mechanical properties of additively manufactured AlSi10Mg_200C using recycled powder." *Materials Science and Engineering: A* 707 (2017): 148-158.
184. Sasani, Farnaz, Ali Karimi Taheri, and Majid Pouranvari. "Correlation between microstructure and mechanical properties of AlMg6/CNT-Al composite produced by accumulative roll bonding process: Experimental and modelling analysis." *Materials Science and Engineering: A* 850 (2022): 143559.
185. Prashanth, K. G., H. Shakur Shahabi, Hooyar Attar, V. C. Srivastava, N. Ellendt, V. Uhlenwinkel, J. Eckert, and S. Scudino. "Production of high strength Al85Nd8Ni5Co2 alloy by selective laser melting." *Additive Manufacturing* 6 (2015): 1-5.
186. Haghdadi, Nima, Majid Laleh, Maxwell Moyle, and Sophie Primig. "Additive manufacturing of steels: a review of achievements and challenges." *Journal of Materials Science* 56, no. 1 (2021): 64-107.
187. Chen, Ying, Chuangwei Xiao, Shang Zhu, Zhiwen Li, Wenxin Yang, Feng Zhao, Shengfu Yu, and Yusheng Shi. "Microstructure characterization and mechanical properties of crack-free Al-Cu-Mg-Y alloy fabricated by laser powder bed fusion." *Additive Manufacturing* 58 (2022): 103006.
188. Szost, B., X. Wang, D. Johns, S. Sharma, A. T. Clare, and I. A. Ashcroft. "Spatter and oxide formation in laser powder bed fusion of Inconel 718." *Additive manufacturing* 24 (2018): 446-456.
189. Nicoletto, Gianni. "Influence of rough as-built surfaces on smooth and notched fatigue behavior of L-PBF AlSi10Mg." *Additive Manufacturing* 34 (2020): 101251.
190. Siddique, Shafaqat, Muhammad Imran, and Frank Walther. "Very high cycle fatigue and fatigue crack propagation behavior of selective laser melted AlSi12 alloy." *International Journal of Fatigue* 94 (2017): 246-254.

191. Uzan, Naor Elad, Shlomo Ramati, Roni Shneck, Nachum Frage, and Ori Yeheskel. "On the effect of shot-peening on fatigue resistance of AlSi10Mg specimens fabricated by additive manufacturing using selective laser melting (AM-SLM)." *Additive Manufacturing* 21 (2018): 458-464.
192. Aboulkhair, Nesma T., Ian Maskery, Chris Tuck, Ian Ashcroft, and Nicola M. Everitt. "Improving the fatigue behaviour of a selectively laser melted aluminium alloy: Influence of heat treatment and surface quality." *Materials & Design* 104 (2016): 174-182.
193. Tang, Ming, and P. Chris Pistorius. "Oxides, porosity and fatigue performance of AlSi10Mg parts produced by selective laser melting." *International Journal of Fatigue* 94 (2017): 192-201.
194. Mordike, B. L. "Creep-resistant magnesium alloys." *Materials Science and Engineering: A* 324, no. 1-2 (2002): 103-112.
195. Mfusi, Busisiwe J., Ntombizodwa R. Mathe, Lerato C. Tshabalala, and Patricia AI Popoola. "The effect of stress relief on the mechanical and fatigue properties of additively manufactured AlSi10Mg parts." *Metals* 9, no. 11 (2019): 1216.
196. Polmear, I. J. "Aluminium Alloys--A Century of Age Hardening." In *Materials forum*, vol. 28, no. 1-14, p. 13. 2004.
197. Cvetkovski, Krste. *Influence of thermal loading on mechanical properties of railway wheel steels*. Chalmers Tekniska Hogskola (Sweden), 2012.
198. Konda Gokuldoss, Prashanth, Sri Kolla, and Jürgen Eckert. "Additive manufacturing processes: Selective laser melting, electron beam melting and binder jetting—Selection guidelines." *materials* 10, no. 6 (2017): 672.
199. Kushwaha, Amanendra K., Merbin John, Manoranjan Misra, and Pradeep L. Menezes. "Nanocrystalline Materials: Synthesis, Characterization, Properties, and Applications." *Crystals* 11, no. 11 (2021): 1317.
200. Khanna, Navneet, Kishan Zadafiya, Tej Patel, Yusuf Kaynak, Rizwan Abdul Rahman Rashid, and Ana Vafadar. "Review on machining of additively manufactured nickel and titanium alloys." *Journal of materials research and technology* 15 (2021): 3192-3221.
201. Ferreira, Daniel FS, G. Miranda, Filipe J. Oliveira, and José M. Oliveira. "Conventionally and SLM-manufactured 18Ni300 steel: mechanical and tribological behaviour in dry sliding against PP40 composite." *The International Journal of Advanced Manufacturing Technology* (2022): 1-14.
202. Bagherifard, Sara, Niccolò Beretta, Stefano Monti, Martina Riccio, Michele Bandini, and Mario Guagliano. "On the fatigue strength enhancement of additive manufactured AlSi10Mg parts by mechanical and thermal post-processing." *Materials & Design* 145 (2018): 28-41.
203. Prashanth, K. G., B. Debalina, Z. Wang, P. F. Gostin, A. Gebert, M. Calin, U. Kühn, M. Kamaraj, S. Scudino, and J. Eckert. "Tribological and corrosion properties of Al–12Si produced by selective laser melting." *Journal of Materials Research* 29, no. 17 (2014): 2044-2054.
204. Eriksson, Mikael, Filip Bergman, and Staffan Jacobson. "On the nature of tribological contact in automotive brakes." *Wear* 252, no. 1-2 (2002): 26-36.
205. Godara, A., D. Raabe, and S. Green. "The influence of sterilization processes on the micromechanical properties of carbon fiber-reinforced PEEK composites for bone implant applications." *Acta Biomaterialia* 3, no. 2 (2007): 209-220.
206. Wang, Jun, Zengxi Pan, Kristin Carpenter, Jian Han, Zhiyang Wang, and Huijun Li. "Comparative study on crystallographic orientation, precipitation, phase transformation and mechanical response of Ni-rich NiTi alloy fabricated by WAAM at elevated substrate heating temperatures." *Materials Science and Engineering: A* 800 (2021): 140307.
207. Wu, Jing, X. Q. Wang, Wei Wang, M. M. Attallah, and M. H. Loretto. "Microstructure and strength of selectively laser melted AlSi10Mg." *Acta Materialia* 117 (2016): 311-320.

 doi:10.20944/preprints202209.0459.v1

208. Zhang, Jinliang, Jianbao Gao, Bo Song, Lijun Zhang, Changjun Han, Chao Cai, Kun Zhou, and Yusheng Shi. "A novel crack-free Ti-modified Al-Cu-Mg alloy designed for selective laser melting." *Additive Manufacturing* 38 (2021): 101829.
209. Deja M, Siemiątkowski M, Zieliński D. "Multi-criteria comparative analysis of the use of subtractive and additive technologies in the manufacturing of offshore machinery components." *Polish Maritime Research*, 27(2020), 71-81.
210. Wang, Zhi, Raghunandan Ummethala, Neera Singh, Shengyang Tang, Challapalli Suryanarayana, Jürgen Eckert, and Konda Gokuldoss Prashanth. "Selective laser melting of aluminum and its alloys." *Materials* 13, no. 20 (2020): 4564.
211. Deja M, Zieliński D, Kadir AZA, Humaira SN. "Applications of Additively Manufactured Tools in Abrasive Machining—A Literature Review." *Materials*, 14,( 2021): 1318.
212. Humaira Mazlan S N, Abdul Kadir A Z, Deja M, Zieliński D, Alkahari M R. "Development of Technical Creativity Featuring Modified TRIZ-AM Inventive Principle to Support Design for Additive Manufacturing". *Journal of Mechanical Design*, 144, (2022): 052001.
213. Walczak M, Szala M. "Effect of shot peening on the surface properties, corrosion and wear performance of 17-4PH steel produced by DMLS additive manufacturing". *Archiv.Civ.Mech.Eng*, 21, (2021): 157.
214. Macek W, Martins RF, Branco R. "Fatigue fracture morphology of AISI H13 steel obtained by additive manufacturing." *Int J Fract*, 235, (2022): 79–98.